Journal of Structural Geology 30 (2008) 1466–1488

Contents lists available at ScienceDirect

Journal of Structural Geology

journal homepage: www.elsevier.com/locate/jsg

Late Proterozoic reconstructions of North-West Scotland and Central Canada: Magnetic fabrics, paleomagnetism and tectonics

Graham J. Borradaile*, Ieva Geneviciene

Faculty of Science, Lakehead University, Thunder Bay, Ontario P7B 5E4, Canada

ARTICLE INFO

Article history:
Received 1 January 2008
Received in revised form 23 July 2008
Accepted 25 July 2008
Available online 6 August 2008

Keywords:
Paleomagnetism
AMS
Torridonian
Scotland
Laurentian
Rodinia reconstruction

ABSTRACT

Red-beds dominate the Stoer Group and the unconformably overlying Torridon Group, having accumulated between ~1400 and ~1000 Ma, in a rift of the Hebridean foreland. The sequences were weakly strained and shortened E–W, and each underwent successive diagenetic changes which altered their magnetic properties and caused their different characteristic post-depositional magnetizations. Anisotropy of magnetic susceptibility (AMS) reveals an N–S vertical tectonic foliation superimposed on the bedding-planar AMS sub-fabric. The tectonic AMS sub-fabric was isolated by comparing normalized and non-normalized mean tensors of multiple specimens. The N–S vertical AMS tectonic foliation postdates warps of bedding; thus the high-susceptibility minerals, including those carrying palaeomagnetic signals re-oriented or recrystallized after deposition and diagenesis. Thus characteristic remanence vectors (ChRM) were acquired long after deposition, first in the Stoer Group, then in the Torridon. ChRMs were isolated for 143 Stoer specimens and 94 Torridon specimens using two cycles of low-temperature demagnetization followed by at least 12 steps of thermal demagnetization. For the Stoer Group, two structurally integral groups of sites yield mean magnetizations of 317.0/+43.1 $\alpha_{95}=11.3$ ($n=49$) and 309.9/52.1 $\alpha_{95}=10.6$ ($n=23$). Some Stoer specimens bear a Torridon age overprint 133.3/+525 $\alpha_{95}=9.6$ ($n=19$). The younger Torridon Group yields 138.4/+52.2 $\alpha_{95}=7.4$ ($n=42$); 134.9/+45.5 $\alpha_{95}=16.0$ ($n=15$) and 134.4/+55.1 $\alpha_{95}=11.3$ ($n=19$) from three structurally integral clusters of sites. These late chemical magnetizations postdate bedding warps, faults and tectonic AMS fabrics; they do not warrant local "rigid-body" tilt corrections. However, we restored the ChRM directions for the regional post-Cambrian eastwards tilt which affected the entire foreland from the Lewisian basement to the overlying Proterozoic strata. Paleopoles calculated from the strata's restored vectors were rotated into Laurentian coordinates for comparison with Canadian Proterozoic palaeopoles. The Stoer Group was magnetized in a normal polarity geomagnetic field whereas the Torridon Group was magnetized in a reversed polarity epoch. However, both sequences include at least one polarity transition, indicating long duration chemical magnetizations successfully averaging secular variation. At a minimum, red-bed magnetization processes exceeded 0.1 Ma and may have encompassed several million years. During Stoer Group magnetization, the Hebridean craton was at paleolatitudes of 26–44°N; when the Torridon Group magnetized it was at 23–27°S. Accepting published ages, this defines a minimum southward *latitudinal* displacement rate of 27–40 km/Ma. Restored Stoer Group paleopoles lie in the present-day north-central Pacific Ocean (~190E/25N); corresponding to the Laurentian APWP dated at between 1090 and 1109 Ma. Torridon Group paleopoles lie in the south-central Pacific (~210E/25S) near the poorly documented (<900 Ma) southernmost part of the Laurentian APWP.

1. Introduction

The commonly accepted Proterozoic reconstruction of the Laurentian, SW Greenland (Gardar) and Hebridean cratons is shown in Fig. 1 (Buchan et al., 1996, 2000, 2001, 1993; Irving and McGlynn, 1981; Piper, 2000; Stewart and Irving, 1974; Thomas and Piper, 1992; Weil et al., 1998; Stewart, 2002). Consider the areas north of the Grenville mobile belt, which cooled from its metamorphic climax at ~1000 Ma. There the craton(s) show continental rifts 80–120 km wide with relatively undisturbed Mesoproterozoic rift sequences valuable for paleomagnetic reconstruction (Halls and Pesonen, 1982; DuBois, 1960; Robertson, 1973; Robertson and Fahrig, 1971; Symons et al., 1994; Weil et al., 1998). Stewart (2002) is the most authorative single source on these rocks in the Hebridean craton (NW Scotland); for the Superior craton rifting see Green (1983) and Franklin et al. (1980). In Canada, the rift sequences overly Archean metamorphic basement (>2500 Ma) but

* Corresponding author. Tel.: +1 807 683 0680.
E-mail address: borradaile@lakeheadu.ca (G.J. Borradaile).

0191-8141/$ – see front matter © 2008 Elsevier Ltd. All rights reserved.
doi:10.1016/j.jsg.2008.07.009

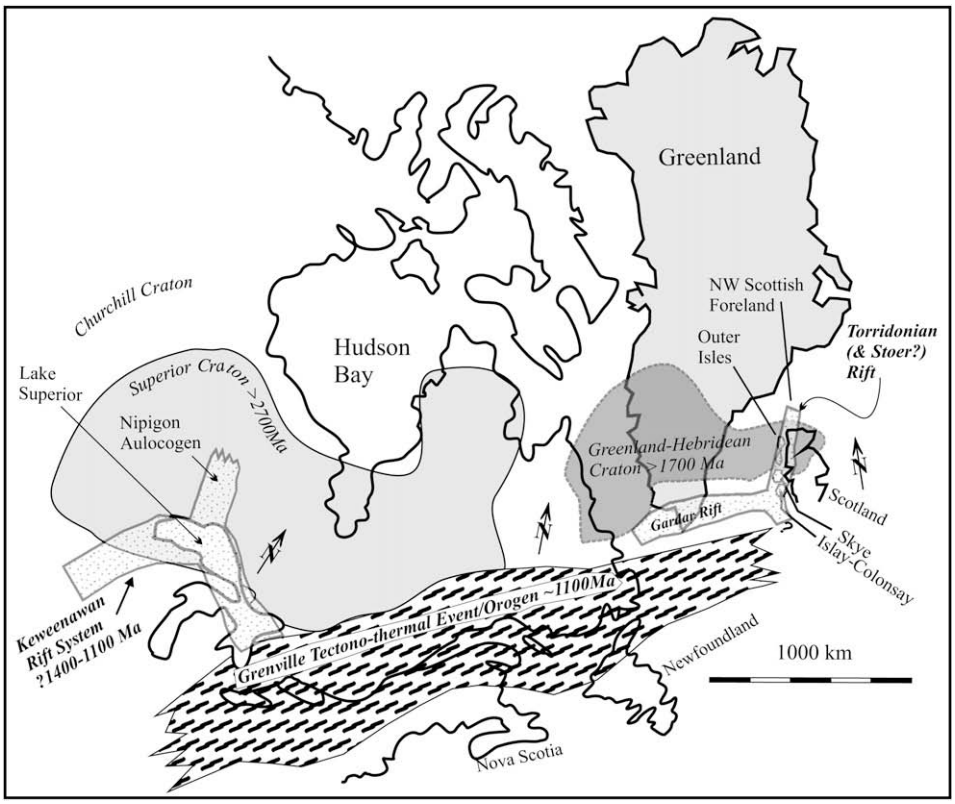

Fig. 1. Present-day landmasses referred to an approximate restoration of Late Archean and Early Proterozoic cratons (Canadian Superior Province and Greenland-Hebridean). These Precambrian Shields lie north of the ~1100 Ma Grenville Mobile Belt. At that time, the principal tectonic effects we discuss are the formation of continental rift sequences along the NW Scottish Foreland (Stoer and Torridon Groups) synchronously with the Gardar Rift, and the triple-junction rift now located in the Lake Superior region. Proterozoic regional geology for the Superior rift sequences is described by Franklin et al. (1980) and Green (1983); and for Hebridean rift by Stewart (2002).

in the Hebridean craton the Archean (Scourian) is mostly reworked by the Inverian and Laxfordian events (1900–1700 Ma). The northern and southern margins of the Superior craton were re-activated in approximately the same time interval by the Hudsonian and Penokean tectono-thermal events, respectively. Recently, Kinnaird et al. (2007), challenge the view that the Torridonian, and perhaps Stoer Groups are preserved in ancient rifts although the nature of their arguments is not clear.

In central Canada and USA, a triple-rift junction formed on the Superior craton between approximately 1500 and 900 Ma (Green, 1983; Franklin et al., 1980; Paces and Miller, 1993; Sutcliffe, 1991), providing a deep basin for shallow water continental deposits, especially red-beds, thick volcanic sequences and sub-volcanic igneous rocks, overlying older Proterozoic sequences (Franklin et al., 1980; Holm et al., 1998). In NW Scotland, thick deposits of shallow water sediment accumulated (~1200 to 990 Ma) in a paleo-rift that approximately follows the course of the Minch channel along the NW Scottish coast. In both regions these depositional basins are bounded by normal faults, although in NW Scotland, the eastern margin of the rift is obscured at the surface by the Caledonian orogenic front, in particular end-Silurian Moine over-thrusting (~430 Ma). In both regions, Proterozoic sedimentary rocks are characterized by lacustrine and fluvial environments featuring red-beds. Fortunately for paleomagnetic study both regions essentially escaped penetrative tectonic deformation (Fig. 1). In NW Scotland, the Proterozoic red-bed sequences escaped Caledonian orogenesis (≥420 Ma) although its tectonic front lies only ~10 km east of the Proterozoic paleo-rift. Absence of significant penetrative deformation permits the red-bed strata to be de-tilted and thus the original orientations of their characteristic magnetizations (ChRMs) to be retrieved. Although restorations for tilts are commonplace, some caution is still required since any history of significant stress or even sub-cleavage finite strains (<8% shortening; Borradaile, 1997) may demagnetize or remagnetize.

The NW Scottish Proterozoic rift basin approximately occupies the Minch Strait between the mainland and the Outer Hebrides. Principally, and specifically in the area we examine, two successive shallow water sedimentary Groups are dominated by red sandstone, unconformable upon the Lewisian gneissic basement. For the Stoer Group, old detrital zircon (3.0–2.55 Ga; Rainbird et al., 2001) was derived from the Lewisian basement, and does not help constrain a maximum depositional age. However, Downie (1962) found Mesoproterozoic nannofossils ("Riphean" 1350–1050 Ma) and Turnbull et al. (1996) suggest a minimum Pb–Pb limestone depositional age of 1199 ± 70 Ma. For example, Stewart (2002) shows that the Stoer Group is overlain with angular unconformity by the Torridon Group. The latter yields a minimum Rb–Sr age of 997 ± 39 Ma from diagenetic phosphate (Turnbull et al., 1996) and a maximum depositional age of 1060 ± 18 Ma from detrital zircon (Rainbird et al., 2001). The radiometric ages are possibly considerably younger than deposition U–Pb Concordia ages (precision ±0.3%) serendipitously provided by more suitable lithologies for the Later Proterozoic Canadian and Gardar cratons (Davis and Sutcliffe, 1985; Green, 1983; Paces and Miller, 1993; Piper, 1987, 1992a,b). As in Central Canada, the Scottish rift system appears to have acted as a repository for continental sediment from ~1400 Ma to the onset of the Grenville tectonic event (~1000 Ma).

2. Microstructure and tectonics relevant to paleomagnetism

Field and micro-structural investigations of the Stoer and Torridon Group sedimentary rocks of the Stoer peninsula (Fig. 2) fail to find convincing macroscopic cleavage. However, pressure solution and strain-shadowing of clasts indicate E–W shortening about

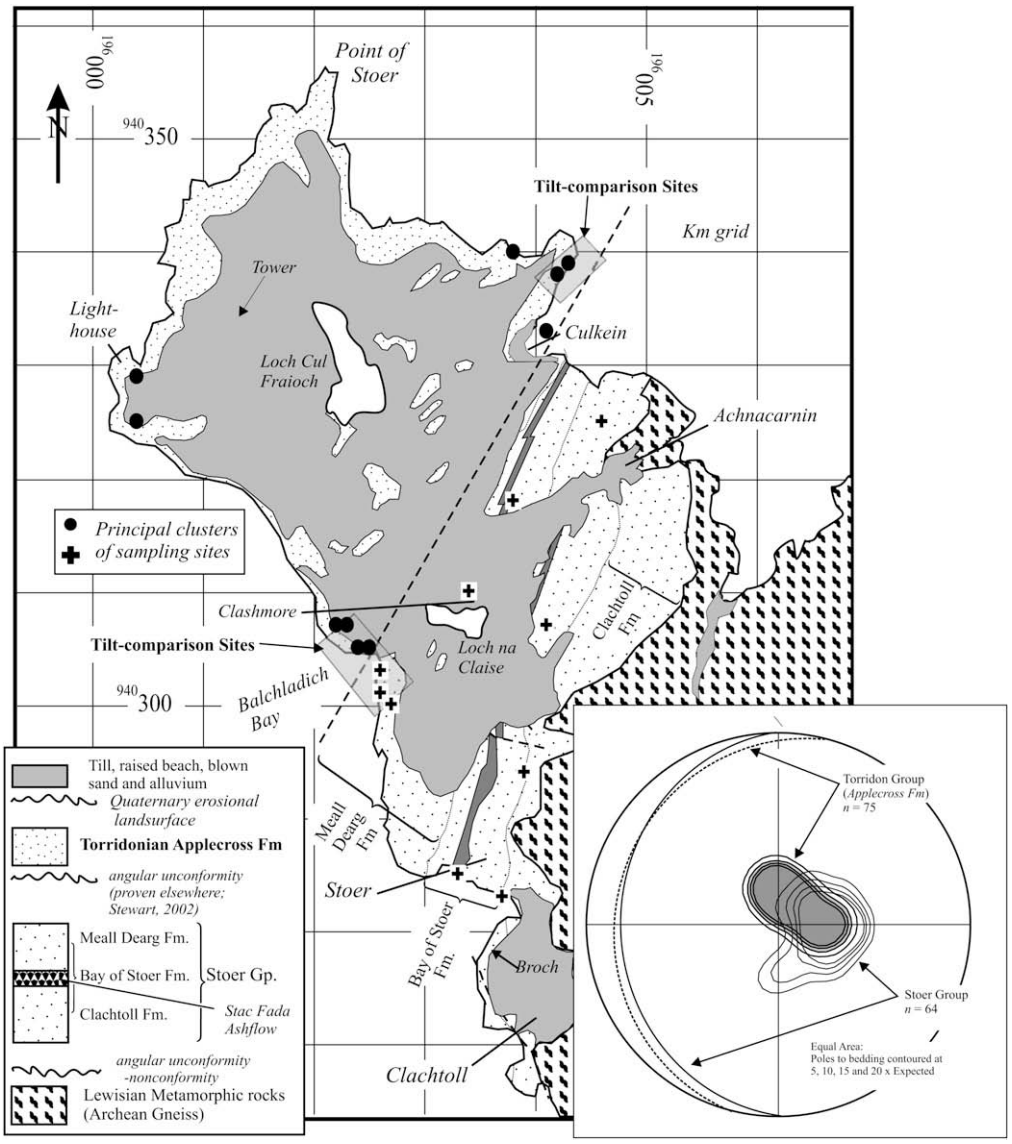

Fig. 2. Principal sampling area and type localities for the Stoer and Torridon Group red-bed sequences and the Stac Fada ash flow, within the Stoer Group (Stewart, 2002). Inset: orientation distribution of bedding planes.

a vertical plane. (Grains with inherited fabrics from the Lewisian basement were obviously excluded.) Quartz grain contacts are sutured due to incipient pressure solution and pressure solution overgrowths occur, both in orientations compatible with E–W layer-parallel shortening. Bedding-parallel mica and chlorite is kinked to be shortened along E–W axes, feldspar clasts show deformation-twinning initiated at grain contacts whereas quartz clasts show sub-grain development around their margins. From our experience of field strain analysis and laboratory experimental deformation, finite strains associated with these micro-structural features are compatible with a shortening of $<10\%$. However, such strains are quite sufficient to trigger remagnetization of magnetite or hematite in the contemporary geomagnetic field, as shown by field and laboratory studies (Borradaile, 1991a,b, 1993, 1996, 1997; Borradaile and Jackson, 1993; Jackson et al., 1993; Robion and Borradaile, 2001; Werner and Borradaile, 1996). The effects of stress-remagnetization are largely unpredictable since small finite strains or ephemeral stress selectively removes specific remanence components of different coercivity in different minerals (op.cit.). Only rarely does a remanence vector spin, controlled only by strain, as would a passive or rigid marker predicted by continuum mechanics (Borradaile, 1993, 1997). Remanence is carried at the submicroscopic level in domains whose stability is dictated by crystal defects; it is not uniformly distributed nor locked inside freely rotating grains (Borradaile, 1997; Dunlop and Özdemir, 1997).

3. Stoer and Torridon Group magnetic mineralogy

Magnetic fabric interpretation is rarely straightforward and is commonly over-simplified; thus some preface is warranted. The response of material to induced magnetization is quantified by the property susceptibility (k). All materials possess a weak diamagnetic susceptibility component (usually near -14×10^{-6} SI or -14 μSI). Diamagnetic magnetization is induced antiparallel to the applied field during its application and unless a rock only comprises *pure* diamagnetic minerals (e.g., quartz, feldspar, calcite), it may be ignored in comparison to the *paramagnetic* magnetization which is large and in the same direction as the applied field. Paramagnetic magnetization thus yields a positive value for susceptibility, several hundred μSI for pure clay minerals and micas, ranging up to 2000 μSI for some pure mafic silicates. In practice these rock forming minerals are not pure and have much higher positive

susceptibilities due to the presence of iron oxides, especially inclusions or exsolutions of magnetite ($\kappa \sim 2.5$ SI) and hematite ($\kappa \sim 0.01$ SI). Magnetite and hematite are the most common remanence-bearing minerals (RBM); a subgroup within the paramagnetic group in which magnetic ordering is retained after the removal of a moderate applied field. To measure susceptibility in a reproducible manner, avoiding any permanent remagnetization, we use a low applied field similar to the magnitude of the earth's field. Much use is made of the anisotropy of low field magnetic susceptibility (AMS) in structural geology because this provides a very sensitive measure of the degree of preferred orientation of minerals. Of course, this is complicated when there are mineral species of very different bulk susceptibility, of different anisotropy or of different orientation distribution (Borradaile and Jackson, 2004).

Bulk susceptibility (κ) was determined by averaging the seven different susceptibility measurements along different axes during AMS measurement (Fig. 3a). The Stoer Group, being most directly derived from the high-grade metamorphic basement is 10 times more susceptible than the Torridonian group due to the enrichment of less weathered magnetite. Despite large susceptibility-differences between hematite ($\sim$0.01 SI) and magnetite ($\sim$2.5 SI), giving a ratio ratio 1: 2500, one must consider their relative abundances. Nevertheless, the bimodal distribution of k, within each group also indicates magnetite–hematite contrasts, probably due to palaeoclimate (Fig. 3a).

Obviously, remanence-properties isolate and characterize the response of RBMs. We studied the acquisition of isothermal remanence using a Sapphiremagnetics SI-6 pulse magnetizer (to 1.2 T) and then studied its decay due to alternating field demagnetization using a Sapphiremagnetics SI-4 AF demagnetizer (maximum peak AF 180 mT) (Fig. 3b). Magnetite very quickly saturates its remanent magnetization as shown by the Stac Fada Ash Flow in the Stoer Group; however, failure to saturate also indicates the presence of hematite. AF demagnetization curves show the characteristic manner by which remanence decays for different minerals. Hematite dominates in the Stoer and Torridon Group sandstones, slowly but incompletely AF demagnetizing to 180 mT. Magnetization, which proceeds to higher fields than is possible by AF demagnetization due to technical feasibility, reveals that no saturation is possible below 1000 mT. This is typical for hematite.

The temperature at which a saturation remanent magnetization is lost also characterizes RBMs. For this we used a Sapphiremagnetics horizontal-translation Curie balance to define critical or Curie-temperatures (T_C) (Fig. 3c–e). All specimens show the presence of hematite ($T_C \sim 670\,^{\circ}$C). However, magnetite ($T_C \sim 580\,^{\circ}$C) dominates in the Stoer Group sandstones and in its Stac Fada Ash Flow. Magnetite may be barely detected in the specimens of Torridon sandstone that we selected. Lower temperature inflexion points near 200 °C and near 320 °C may be due to titanomagnetite and pyrrhotite respectively, or to oxidized titanomaghemites.

4. Magnetic fabrics

Anisotropy of magnetic susceptibility (AMS) measured in a low alternating field merges the induced magnetization contributions of all minerals. This incorporates responses of different minerals, their abundances, their bulk susceptibility and their mineral-anisotropy (Hrouda, 1982; Borradaile and Henry, 1997; Borradaile and Jackson, 2004; Borradaile, 1988). The interpretation requires us to at least qualitatively balance the abundance of different minerals, considering their different bulk susceptibilities and anisotropies and, in more complex cases, different minerals may possess different orientation distributions (op.cit.) (Fig. 4).

Some low technology approaches permit us to isolate the fabric contribution of different mineral species with different κ (Borradaile, 2001a; Borradaile and Gauthier, 2003). AMS is visualized as a magnitude-ellipsoid for which the radii define the susceptibility value along that axis. The ellipsoid is representation of a second-rank tensor, with principal axes, $k_{MAX} \geq k_{INT} \geq k_{MIN}$. k_{MAX} defines magnetic lineation and, where the ellipsoid shape is appropriate (k_{INT}–k_{MIN}) fixes the magnetic foliation. These values are usually positive, since the most rock forming minerals ($\kappa > 500$ μSI) and iron oxides ($\kappa > 200{,}000$ μSI) are *paramagnetic* at low fields. Although it does not concern us here, it must be noted that some important rock forming minerals, *if pure*, such as quartz, feldspar and calcite have a small negative susceptibility (~ -14 μSI) but their fabric contribution is usually swamped by the paramagnetic minerals (Rochette, 1988; Rochette et al., 1992). Because of these complicating factors, it is widely accepted that principal susceptibility axes may define kinematic or strain axes, but it is highly improbable that they ever define strain magnitudes (Borradaile, 1991b).

Standard AMS specimens (25.4 mm diameter; 22 mm high) typically comprise several hundred mafic silicate grains with $\kappa \geq 500$ μSI so that they dominate specimen-AMS. However, depending on their abundance, accessory RBM may pose interpretative problems (Fig. 4). For example, traces of magnetite ($\kappa \sim 2.5$ SI) as independent grains or inclusions may suffice to swamp the anisotropy signal from a paramagnetic matrix. Moreover, magnetite's high susceptibility causes its AMS to be shape-controlled, not crystallographically controlled as with all other minerals. Since the shape-orientation distributions of magnetite grains and silicate crystals may differ, their blended contribution in the rock-AMS signal may not faithfully represent either mineral fabric. Blended sub-fabrics may be isolated (on separate stereograms) by comparing AMS orientations for sub-samples of different κ (bulk susceptibility) (Borradaile and Gauthier, 2003) or by comparing normalized and non-normalized mean tensors (Borradaile, 2001a). Of course, laboratory techniques of varying sophistication also permit one to physically isolate different sub-fabric contributions from different minerals (Borradaile et al., 1987; Jackson, 1991). Unfortunately, they are not appropriate for all rocks, including those studied here.

4.1. Some principles of interpretation of magnetic fabric

The AMS of most rocks blends contributions of susceptibility anisotropy of different minerals, in some cases with different orientation distributions (subfabrics). The degree to which each mineral and each subfabric influences the net rock AMS depends on the mean susceptibility of each mineral species and on its abundance (Borradaile et al., 1990; Borradaile, 1987; Borradaile and Jackson, 2004; Henry, 1989; Rochette, 1987, 1988; Rochette et al., 1992). Consider the range of AMS ellipsoid shape for a specimen blending high anisotropy matrix silicates and lower anisotropy but high-susceptibility magnetite (Fig. 6a). Using Jelinek's (1978) parameters, P_j ranges from 1.0 (sphere) upward on a logarithmic scale whereas shape is represented by T_j (+1, oblate; −1, prolate). Fig. 6b models the AMS of a rock dominated by two highly susceptible minerals of different anisotropy; magnetite and phlogopite are shown over an extreme range of mixing values. More importantly, changes in the concentration, susceptibility and mineral-AMS of different minerals affect the overall specimen's AMS axial directions. For example, the maximum susceptibility (k_{MAX}) due to two different orientation sub-fabrics of magnetite traces in a phlogopite matrix may be parallel to the phlogopite alignment for 1 ppm magnetite but effectively parallel to the magnetite alignment if its concentration rises to 100 ppm (Fig. 4).

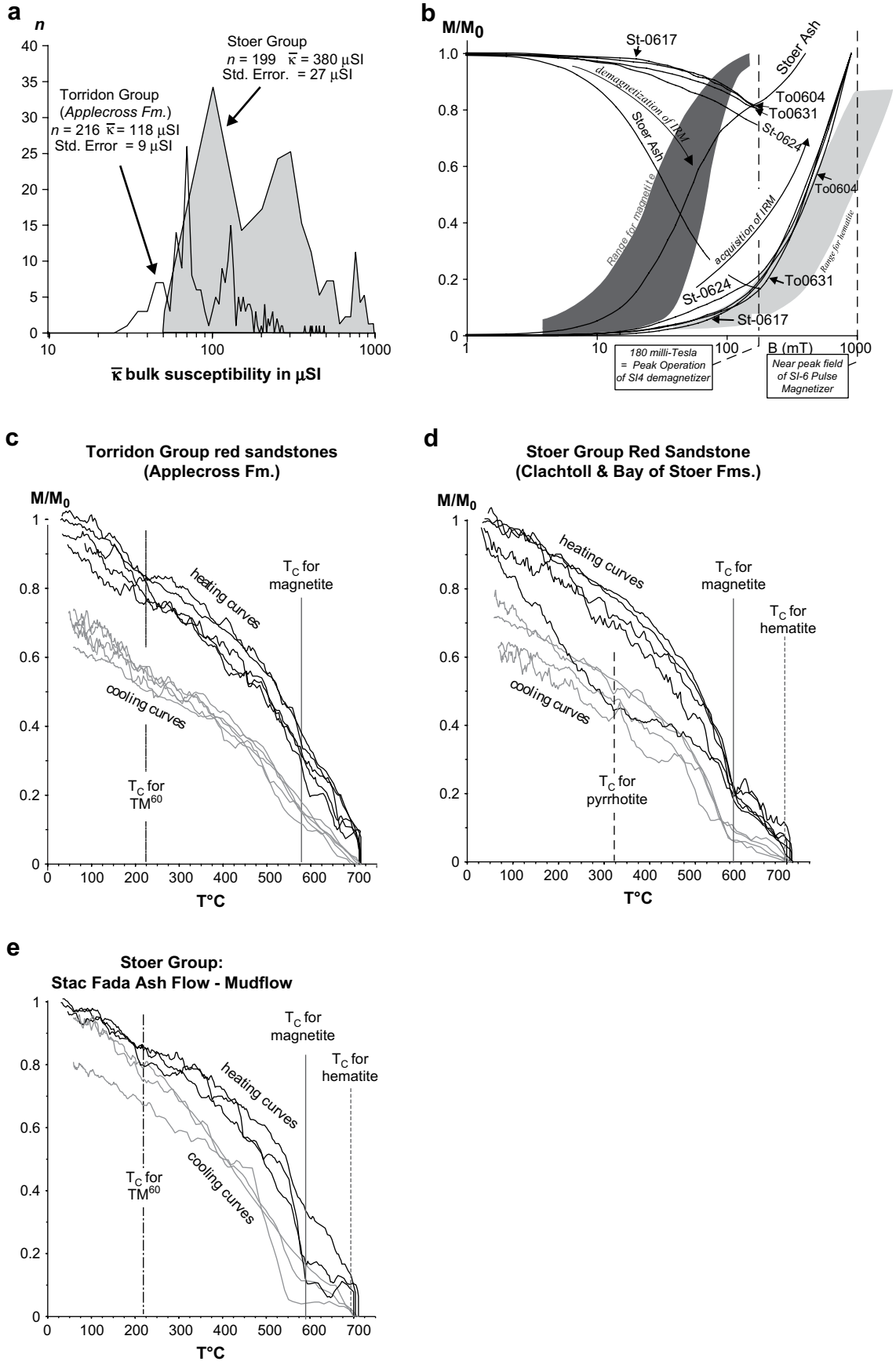

Fig. 3. (a) Frequency distribution of bulk susceptibility (log scale) for the red-beds of the Stoer and Torridon Group sedimentary rocks of the Stoer peninsula. (b) Acquisition of isothermal remanent magnetization (IRM) and its progressive demagnetization by alternating fields (AF). Shaded regions show Dunlop's (1972) ranges for pure magnetite and pure hematite. (c–e) Thermomagnetic curves obtained with Sapphiremagnetics horizontal–translational Curie Balance. Heating curves are shown darker than cooling curves.

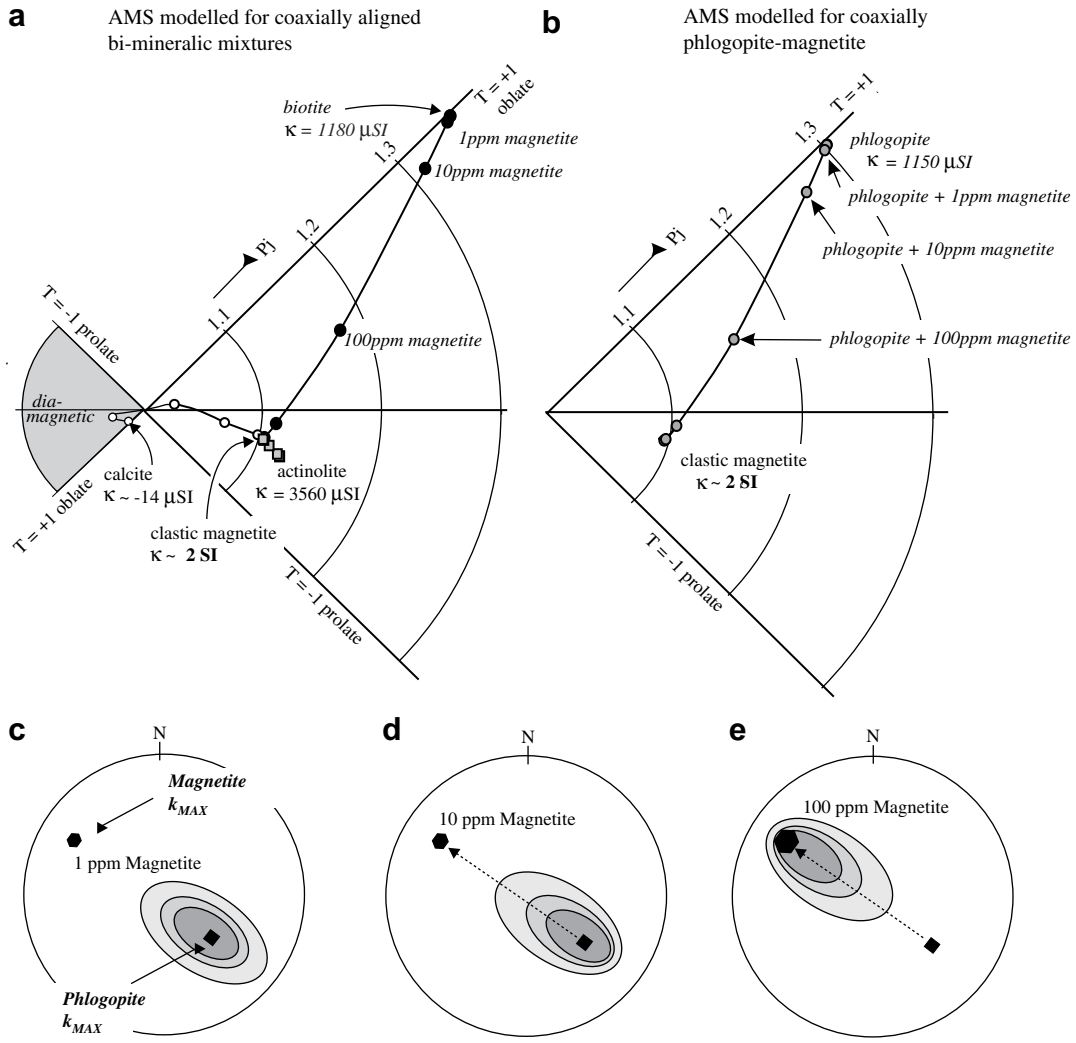

Fig. 4. Interpretation of the anisotropy of magnetic susceptibility, in terms of magnetic petrofabric requires an evaluation of the relative roles of anisotropy and bulk susceptibility. (a–b) Magnetite, although present in traces has such high susceptibility that its low (shape-controlled) anisotropy may control the AMS ellipsoid's shape despite the fact that the matrix silicates may have much higher (crystallographic controlled) susceptibility anisotropy. (c–d) More importantly, this balance principle affects the orientation of the AMS ellipsoid's axes; increasing trace concentrations of high-susceptibility magnetite shift the specimen's maximum susceptibility towards that of the magnetite and away from that of the silicate matrix which may be differently oriented.

Laboratory techniques may non-destructively, isolate the orientation distribution of magnetite (or other RBM) from the orientation distributions of matrix paramagnetic/diamagnetic minerals which is commonly necessary in strained or metamorphic rocks (Nakamura and Borradaile, 2001a,b; 2004). The techniques AARM (anisotropy of anhysteretic remanence; Jackson, 1991) or AIRM (anisotropy of isothermal magnetization; Daly and Zinsser, 1973) are demanding laboratory techniques limited to RBM of suitable coercivity ranges. For example, these Scottish Redbeds are unsuitable for the study of remanence anisotropy because the coercivity of hematite is too high to permit the removal and reapplication of experimental remanences in different directions.

The alternative, data-processing approaches are moderately effective at isolating different orientation distributions if the minerals have sufficiently different κ. The simplest approach plots and compares separate orientation distributions for high-susceptibility (magnetite-rich) *versus* low susceptibility specimens (magnetite-poor) (Borradaile and Gauthier, 2003). More rigorously one may compare the mean AMS tensor of the specimens and its confidence regions for a single data-sample, with the same sample after *normalization* (Borradaile, 1993, 2001a, 2003). The normalized mean tensor is simply recalculated by assigning unit-weight to the bulk susceptibility of each specimen. Each specimen thus has "unit-susceptibility" and specimens of high susceptibility do not deflect the mean tensor axes. Suppressing the outlying effects of anomalously high-susceptibility sub-fabrics, or anomalously oriented sub-fabrics has merits and disadvantages, depending on whether one wishes to emphasize the contribution of a certain sub-fabric or suppress it. For example, the Borrowdale Slate AMS is primarily controlled by high anisotropy and moderate susceptibility chlorite, whereas its magnetite traces have low anisotropy and high susceptibility. Fig. 5a reveals the sub-fabric differences from normalized and non-normalized tensors. Two further examples, from the Canadian Shield, reveal how the contribution of magnetite-rich specimens is subdued by normalization, better revealing the orientation and symmetry of the matrix (Fig. 5b, c).

Another interpretation problem concerns the significance of principal axes wherever the AMS fabric is not a saturation fabric. Non-saturation fabrics retain some vestige of a primary AMS fabric overprinted with the secondary (tectonic) fabric. Progressive development of the overprinting AMS may cause a switching of the orientations of the principal susceptibility axes during fabric development. This is not caused by (but may accompany) some physical rotation of the axes relative to the material. It is better to

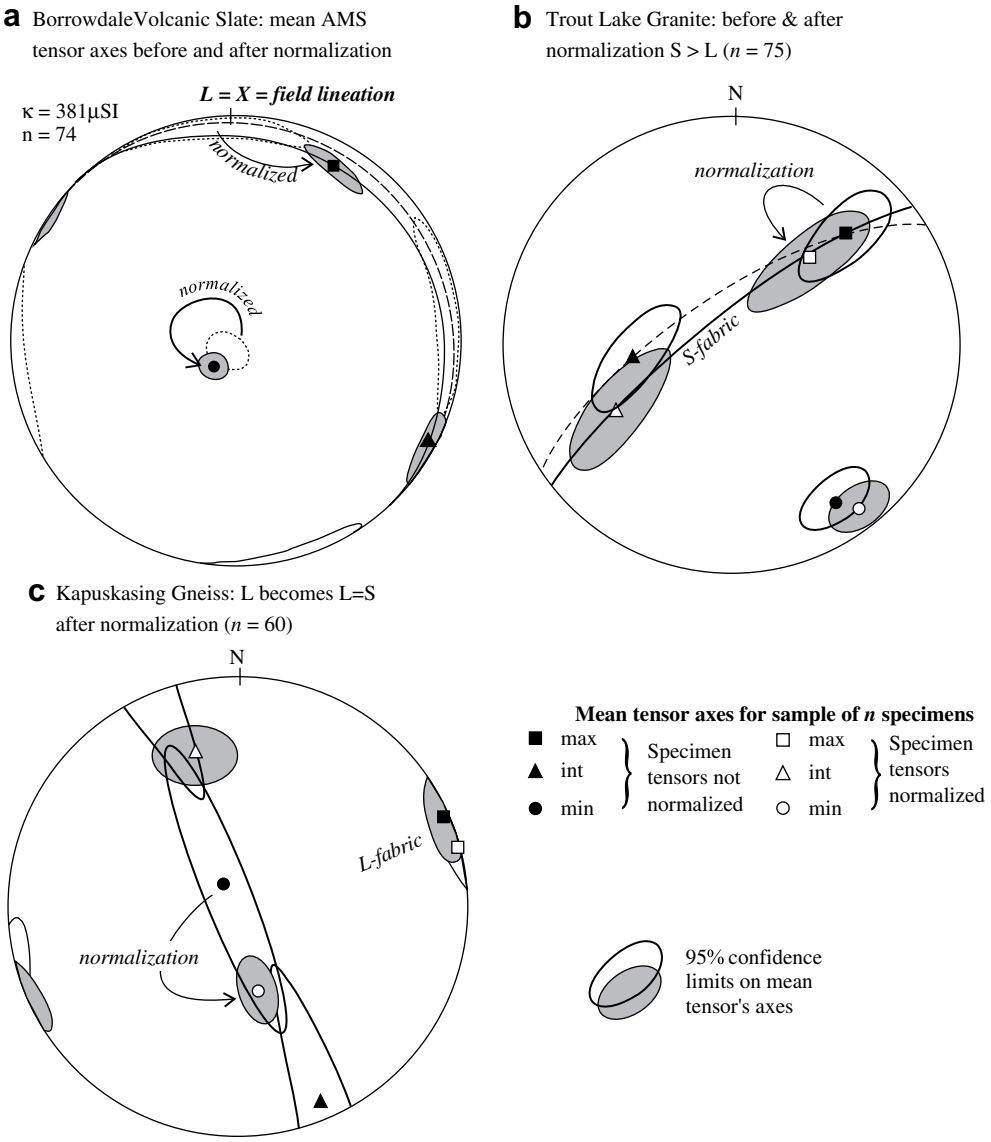

Fig. 5. The relative roles of mineral sub-fabrics with different orientations and different mean susceptibilities may be most efficiently discerned by comparing the mean tensor for the raw sample of specimens with that of the normalized sample. The raw sample AMS is that routinely determined in which each specimen's direction weights the orientation of the mean tensor for all specimens, according to its bulk susceptibility. That is to say, the sample's mean susceptibility axes are shifted towards the orientations of anomalously oriented, high-susceptibility specimens (see Fig. 6). The normalized mean tensor is a re-calculation in which each specimen's AMS is reduced to a unit-ellipsoid by dividing each of its principal susceptibilities (k_{MAX}, k_{INT}, k_{MIN}) by the specimen's mean susceptibility. The raw or non-normalized mean tensor emphasizes the contribution of the high-susceptibility sub-fabric whereas the normalized mean tensor suppresses its importance (Borradaile, 2001a). In these examples of metamorphic rocks, the procedure indicates differently oriented sub-fabrics but it also indicates symmetry differences (i.e. L *versus* S tectonite) from the shape of the confidence regions around the mean tensors' principal axes.

conceive of the principal susceptibility axes (K_{MAX}, etc.) shrinking or growing as the fabric evolves. At some point, the relative magnitudes of pairs of principal axes are exchanged, e.g. Fig. 6a. For example, weakly deformed sedimentary rocks possess a bedding-defined AMS foliation (bedding $\equiv k_{MAX} - k_{INT}$) which commonly transforms into one where k_{MAX} is parallel to a bedding–cleavage-intersection (Fig. 6b) or parallel to a fold axis (Fig. 6c) (Borradaile and Tarling, 1981; Borradaile and Sarvas, 1990). Rochette et al. (1992) and Ferré (2002) studied this more systematically (Fig. 6d).

5. AMS fabrics Stoer peninsula

The Torridonian Applecross Group forms the younger sequence of Proterozoic sandstones on the Stoer peninsula. For low susceptibility sandstones (mean $\kappa = 92$ μSI), the most common magnetic petrofabric defines a depositional-controlled fabric with k_{MAX}–k_{INT} parallel to bedding (Fig. 7a). The 95% confidence regions for k_{MAX} and k_{INT} trace out the bedding plane, indicating the importance of the bedding-parallel fabric and the scatter of mineral long axes in bedding. Their confidence regions are so elongate that the bedding AMS fabric is of the S-type and the actual k_{MAX} direction is too vaguely defined to imply any clear depositional or later tectonic influence. Seven of the 184 specimens shown have anomalous inverse fabrics with k_{MAX} steeply oriented, near the pole to bedding (Fig. 7a). Such examples are probably due to SD magnetite which although aligned parallel to bedding yields an *inverse* AMS fabric (Potter and Stephenson, 1988). AMS ellipsoids are commonly quite eccentric (i.e., large P_j) in depositional fabrics (Fig. 7b) since the primary preferred grain alignment commonly exceeds that in early-stage tectonism (Borradaile and Jackson, 2004; Tarling and Hrouda, 1993). However, AMS fabric shapes are generally neutral ($T_j \sim 1$), midway between the prolate and oblate end-members.

Stoer and Torridon Group AMS data have been regrouped according to mean susceptibility, and also to whether the fabric is

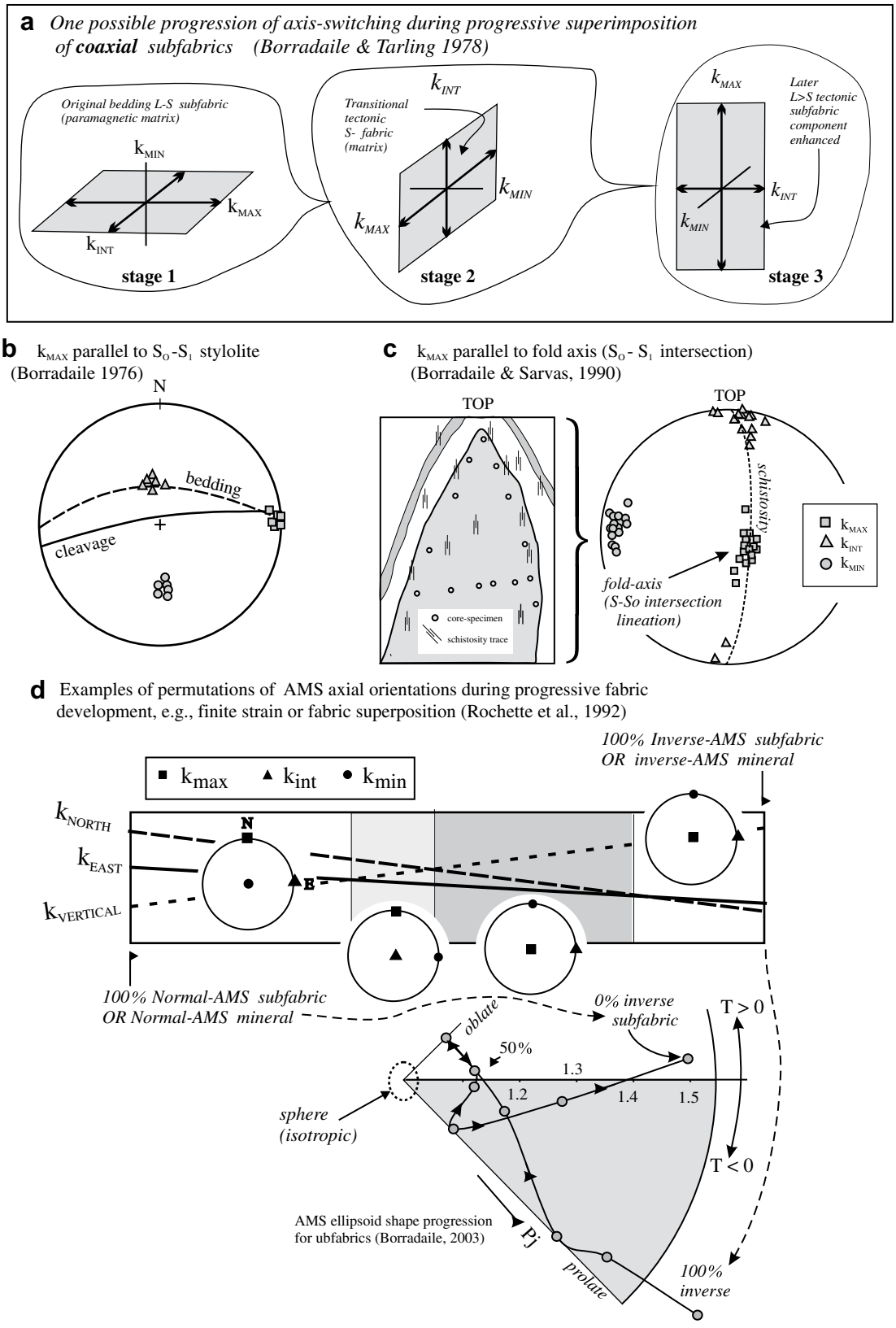

Fig. 6. Counter-intuitive or anomalous AMS axial orientations. (a) Due to progressive superposition and development of a tectonic sub-fabric on a depositional sub-fabric development. (b–d) Producing k_{MAX} (or k_{INT}) parallel to bedding–cleavage-intersection. (e) Due to contributions of inverse AMS minerals (e.g. single-domain magnetite).

bedding-dominant or with some tectonic element (Figs. 8–11). The more susceptible (mean $\kappa = 118$–380 μSI) Torridon sandstones show well-defined subhorizontal k_{MAX}–k_{INT} bedding-foliation with a nearly N–S k_{MAX} from the raw measurements (Figs. 8, 9). However, after normalization, the high-susceptibility specimens that distort the sample towards a bedding-dominant sub-fabric are suppressed. Thus, an NW–SE vertical AMS foliation is revealed with k_{MAX} (lineation) horizontal (~bedding–cleavage-intersection,

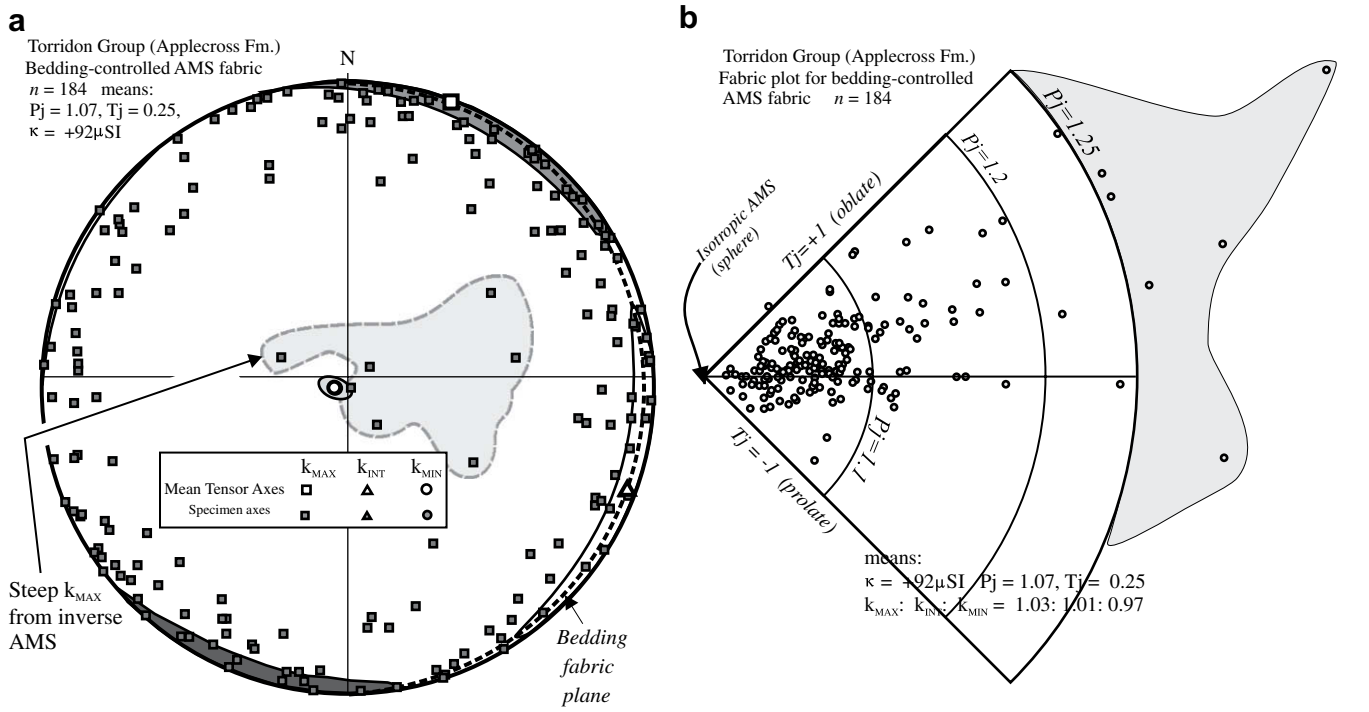

Fig. 7. (a) Depositional-controlled AMS fabric orientations, k_{MIN} perpendicular to nearly horizontal bedding, poorly defined mean k_{MAX} for tensor in bedding plane. Note some specimens have inverse fabrics (e.g., see Fig. 8e) due to single-domain magnetite. (b) AMS ellipsoid shapes show a broad range of anisotropy with most eccentric ellipsoids (large P_j, shaded) associated with single-domain inverse fabrics from (a).

Fig. 6) and k_{INT} vertical (Fig. 8). The Stoer sandstones have a well-defined bedding fabric both without and after normalization (Figs. 8, 9). Their AMS ellipsoid shape distributions are slightly skewed toward oblate but nearly neutral (Fig. 9). A higher susceptibility sub-sample ($\kappa = 570$ μSI) is also unaffected by normalization due to the strong alignment of high-susceptibility magnetite parallel to bedding. A further sub-sample of Stoer sandstones is identified on the basis of AMS orientation and lower mean susceptibility ($\kappa \sim 270$ μSI) (Fig. 9). Non-normalized data reveal an N–S foliation with k_{MAX} horizontal and k_{INT} vertical, typical of a transitional bedding-to-cleavage fabric with k_{MAX} parallel to the intersection lineation. It is notable that the ellipsoid shapes are bi-modally distributed (Fig. 9e), a feature that commonly arises during fabric transition and axis-switching (cf. Fig. 6).

Although it is of limited geographical extent, the Stac Fada Ash flow, within the Stoer Group is of great significance, being the only volcanic rock in the entire rift sequence. On the Stoer peninsula, it is about 10 m thick with clear flow banding and aligned volcanic clasts commonly reaching 30 cm in maximum dimension. Bulk susceptibility is dominated by magnetite but later it will be seen that hematite is equally important to paleomagnetism. AMS fabrics as measured directly (Fig. 10a), define a bedding-parallel k_{MAX}–k_{INT} foliation, with a flow lineation defined by the E–W k_{MAX} axis. This direction concurs with the conclusions of Stewart (2002) on sedimentological and field-geology grounds. Of course, if we process the same directions by normalizing specimen principal susceptibilities by their mean value, the orientation fabric may differ, giving insight into the roles of depositional versus tectonic fabrics (Fig. 13b; Borradaile, 2001a). First, confidence regions for the normalized mean tensor axes are less well defined because the presence of magnetite-rich specimens strongly weighted the mean tensor in (a). In that case, as found in many other volcanic rocks (Tarling and Hrouda, 1993), primary magnetite is probably a good flow-axis indicator. After normalizing (Fig. 10b), the magnetite contribution is subdued and the more scattered (and lower susceptibility) matrix silicates weaken the sense of preferred orientation. Also, the confidence regions of the normalized sample (Fig. 10b) are asymmetric, confirming that two orientation distributions were present.

East of the Stoer peninsula, near Loch Assynt, the Torridon Group sandstones are closer to the Caledonian tectonic front and possibly even lie just east of the eastern paleo-rift margin. The raw AMS orientation distribution and the normalized AMS distribution show consistent tensor-mean orientations (Fig. 11a, b). Orientation-consistency verifies the equal dominance of the high and low susceptibility sub-fabric components and also their similar orientations. However, the symmetry of the tensor-mean confidence regions is somewhat reduced by normalization, indicating some disorientation due to a magnetite sub-fabric was present in the non-normalized mean tensor. Normalization preserves the bedding component (Fig. 11a) but it is defined by k_{MAX}–k_{MIN}, and not by k_{MAX}–k_{INT}, indicating a partial tectonic overprint (cf. Fig. 6a). Thus, the vertical k_{MAX}–k_{INT} foliation defines an embryonic tectonic fabric, a feature recognized in many weakly deformed sedimentary rocks (cf. Fig. 6).

Thus, Stoer and Torridon Group AMS fabrics retain bedding (k_{MAX}–k_{INT}) sometimes with a depositional lineation (k_{MAX}). However, AMS mean tensor normalization may also reveal a partial tectonic overprint in which k_{INT} is nearly perpendicular to bedding with k_{MAX} parallel to bedding, defining an embryonic vertical N–S foliation. This is transitional to some sites where a complete tectonic fabric has a vertical N–S k_{MAX}–k_{INT} foliation. Variations on this sequence have been documented elsewhere (Fig. 6).

6. Paleomagnetism

The techniques of palaeomagnetism and the interpretation of palaeomagnetic data in a structural context are most conveniently described by McElhinny and McFadden (2000). Paleomagnetic investigations of the Scottish Proterozoic Torridon and Stoer Group sedimentary rocks have a long and distinguished history (*inter alia* Irving, 1957; Irving and Runcorn, 1957; Stewart and Irving, 1974;

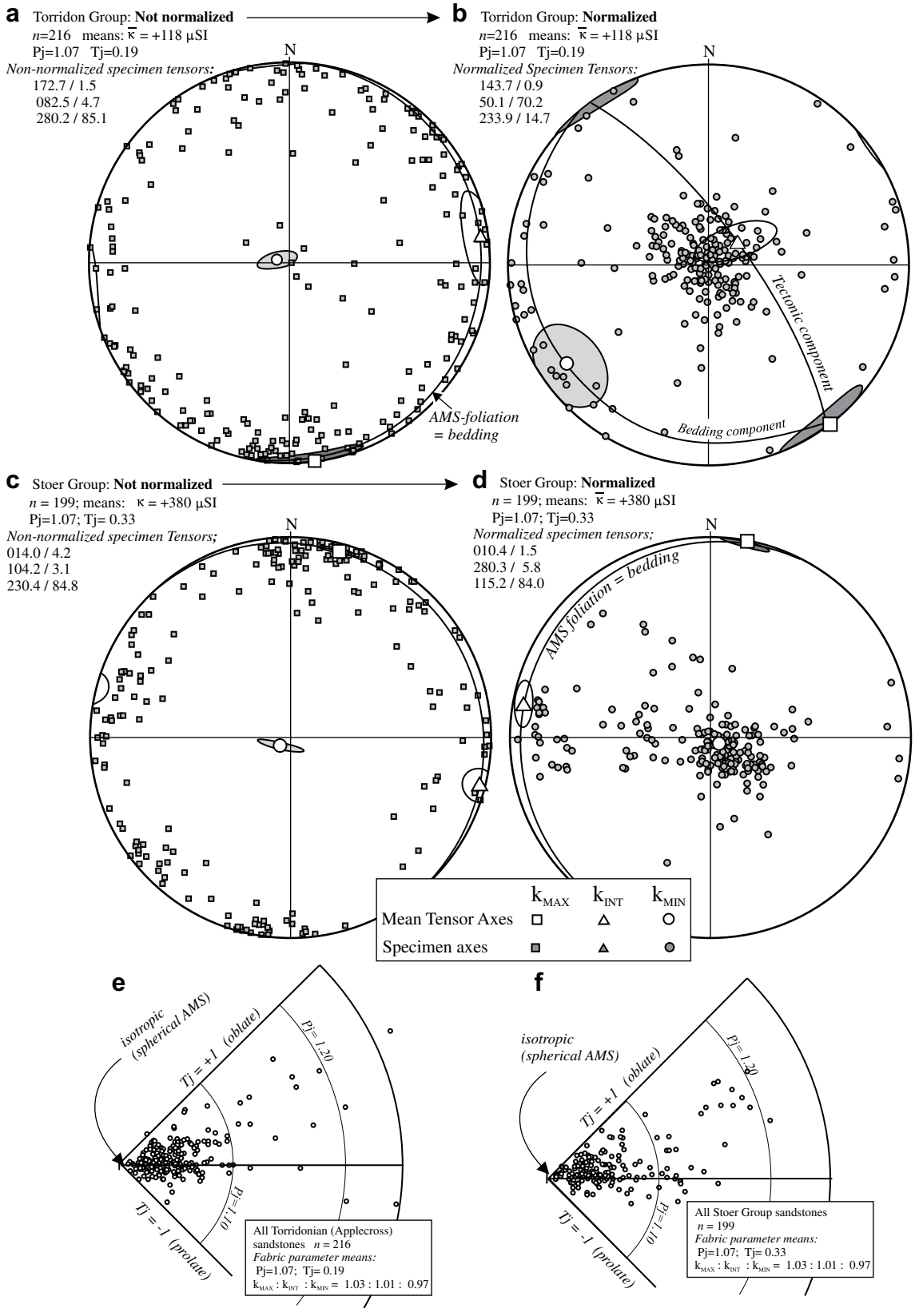

Fig. 8. Normalization of a sample of Torridon Group sandstone specimens in (a) reveals a matrix sub-fabric that is tectonically controlled with an NW–SE steep foliation and NW–SE horizontal magnetic lineation in (b). (c–d) For this sample of Stoer Group sandstones, normalization yields little more information because the high-susceptibility sub-fabric that controls (a) is similarly oriented to the matrix fabric, emphasized by (b). (e–f) These samples of Stoer and Torridon Group sandstones have similar, broad distributions of AMS ellipsoid shapes.

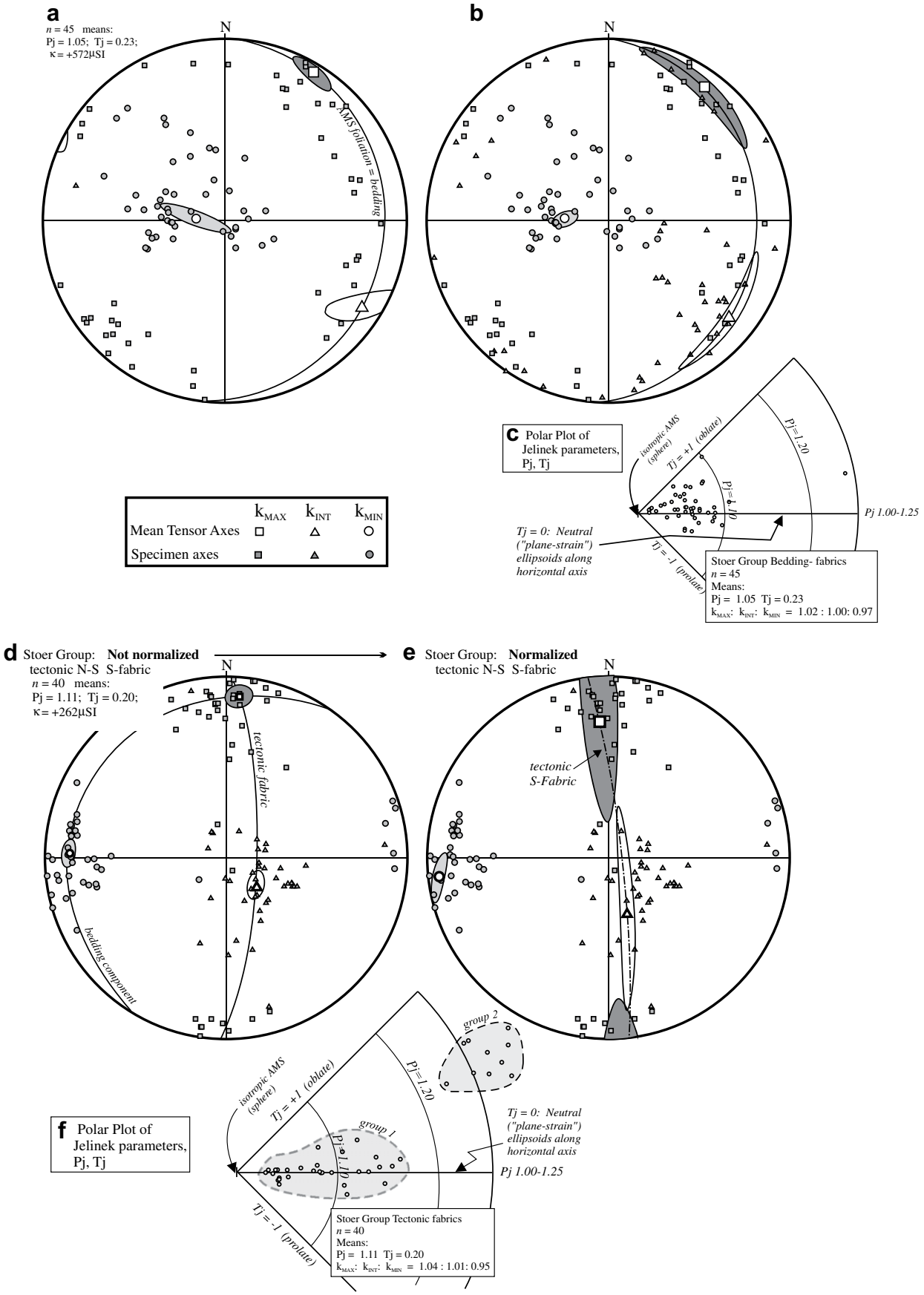

Fig. 9. Normalization (a–b) of a sample of low anisotropy (c) Stoer Group sandstones produces negligible change in the mean tensor orientation (b) due to a strong bedding-controlled sub-fabric. However, normalization (d–e) of a sample of bimodal but high anisotropy (f) Stoer Group sandstones reveals an N–S AMS foliation due to a tectonic sub-fabric of the lower susceptibility matrix minerals.

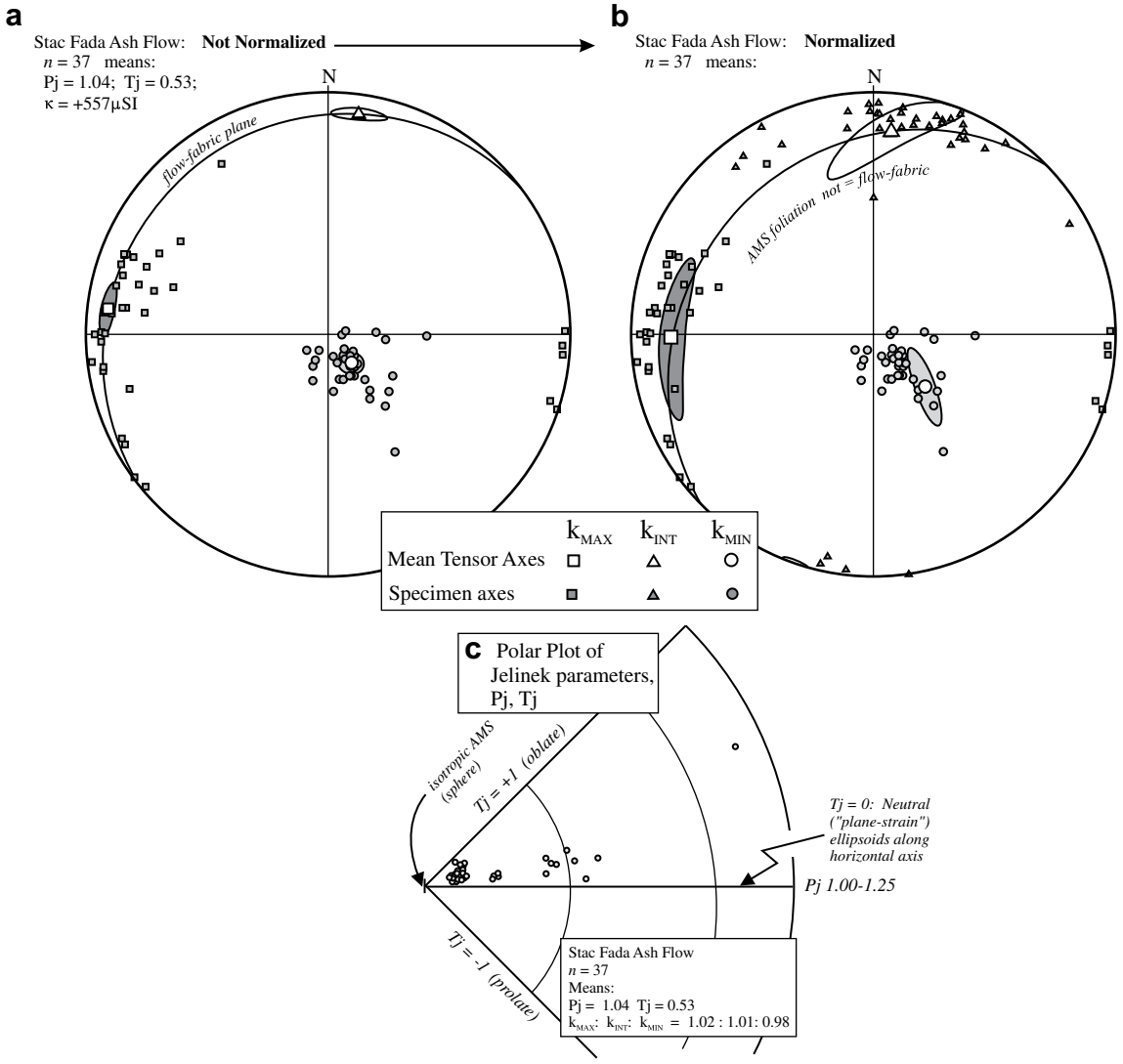

Fig. 10. (a) The Stoer Group's Stac Fada ash flow shows a bedding/flow aligned sub-fabric with an E–W flow axis. (b) Normalization reduces the precision of axial orientation and reduces AMS symmetry. This indicates that the AMS is dominated by the high-susceptibility magnetite sub-fabric of (a) with a less well-defined matrix fabric showing its influence in (b).

Torsvik and Sturt, 1987; Darabi and Piper, 2004; Dulin et al., 2005; Piper and Poppleton, 1991). The most appropriate text to introduce structural geologists to palaeomagnetism is by McElhinny and McFadden (2000). The underlying gneissic basement, Stoer sand-dike penetrations and conglomerate tests of pre-Stoer, Stoer, and post-Torridon clasts have all helped to bracket the two fundamental ChRM directions predominantly as post-depositional chemical remanence in specular hematite. We will show that the ChRMs are accompanied by antiparallel examples due to reversed polarity magnetization. Thus hematite magnetization must considerably postdate deposition and have been acquired over intervals long enough to include polarity transitions of the paleofield ($\geq$0.1 Ma to several Ma.) This verifies the stability and antiquity of the ChRMs (van der Voo, 1993; Table 1). Less than 10 km east of the Stoer peninsula, the Caledonian front yields late Silurian post-tectonic and syntectonic magnetizations with directions that cannot be confused with the directions in the Stoer and Torridon Groups (e.g., Darabi and Piper, 2004; van der Voo, 1993, Table A2). Thus, Caledonian remagnetization is not detected in the Stoer and Torridon rift sequence red-beds. However, Proterozoic rift-fault compressions and dilations have imparted a feeble tectonic AMS with N–S or NW–SE foliation in the Stoer and Torridon Groups as already discussed. Clastic dikes and faults indicate that N–S or NW–SE extension occurred after Stoer deposition and again after Torridon deposition (Dulin et al., 2005).

The paleogeographic importance of the Stoer and Torridon Groups lies in the fact that they are a relatively undisturbed cover sequence on reworked Archean foreland (2200–1700 Ma) that maybe restored within a late Proterozoic paleogeography between the Shields of Laurentia and Baltica. Few such undisturbed and readily restored continental fragments area available. For example, Mesoproterozoic rift sequences in the Laurentian craton (Fig. 1) are tectonically suitable but they are commonly remagnetized by a widespread Keewenawan ($\sim$1000 Ma) hydrothermal event.

Together, the Hebridean craton, the Laurentian craton and the intervening Gardar craton of SW Greenland may be satisfactorily restored using known Euler rotation axes, to reconstitute an important part of the late Proterozoic supercontinent known as Rodinia (Buchan et al., 2001; Piper, 1991, 2000). One of the most vexing problems with the paleomagnetism of ancient rocks is due to the effects of later tectonic deformation. Where this merely causes rigid-body tilting, restorations may be possible (MacDonald, 1980). However, it is rarely possible to restore for the effects of finite strain (Borradaile, 1993, 1997; Borradaile and Mothersill,

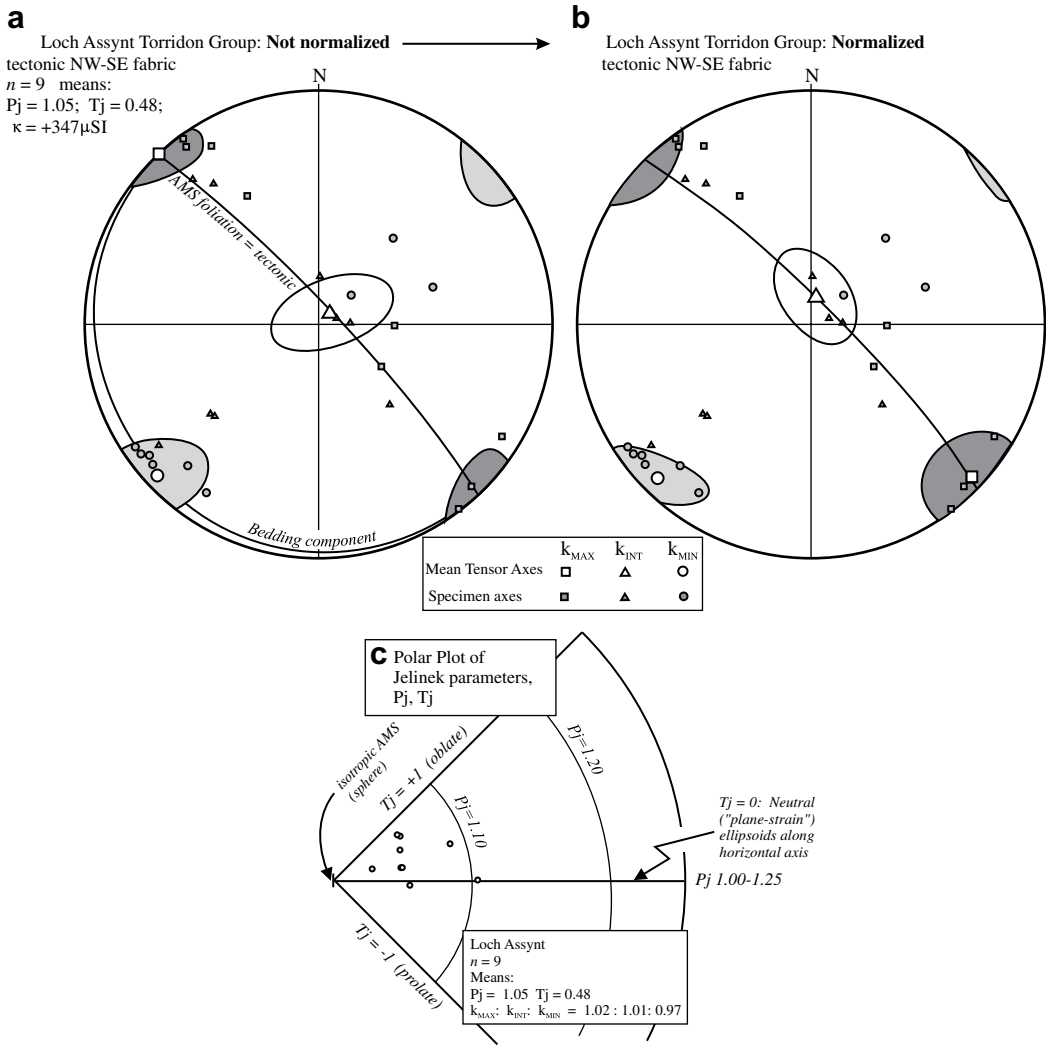

Fig. 11. Approximately 10 km west of the Stoer peninsula, near the east margin of the Proterozoic rift, (a) even raw AMS fabrics reveal an NW–SE tectonic fabric. (b) Normalization enhances the symmetry of this tectonic fabric which nevertheless is of relatively low eccentricity (c).

Table 1
Quality criteria paleomagnetic pole (Modified from van der Voo (1993))

1 Geochronological Age = Magnetization Age.	Most important but rarely perfectly satisfied. A limiting age or age-brackets may be almost just as useful.
2 For single site $n > 24$ & $k \geq 10$ & $A_{95} \leq 16^{\circ}$.[a]	Less stringent criteria may suffice from a group of sites or where several of the following criteria enhance the quality of the data.
3 Complete incremental demagnetization of every specimen.	One or more techniques appropriately selected (Schmidt, 1993).
4 Stability test to bracket or limit magnetization age, relative to a depositional or cooling age.	Fold, conglomerate, baked contact tests (Graham, 1949; Everitt and Clegg, 1962).
5 Presence of intra-formational antiparallel reversals of the paleofield (as represented by ChRMs isolated by consistent demagnetization technique).	Almost as powerful as a stability test (#4 above).
6 Paleopole location differs from younger paleopoles.	Not required but helps.
7 No tectonic strain, and preferably no rigid-body tilting.	Magnetization directions cannot be restored after strain although de-tilting is commonly possible (Borradaile, 1997, 2001b; MacDonald, 1980).
8 Duration of magnetization process: longer processes average effects of secular variation.	Requires petrographic considerations and rock-magnetic work in laboratory.
9 Presence of secular variation within a formation; must correlated with stratigraphy at multiple sites.	Requires well-bedded and correlated strata between sites.

Item l: only perfectly satisfied in rapidly acquired thermal magnetizations, e.g., lava. However, in this case a ChRM samples secular variation and defines a VGP (virtual geomagnetic pole). One must average ChRM directions from many lava flows to cancel secular variation and define a true paleopole. Items 2, 3: these are within the control of the researcher and should always be achievable, given sufficient effort and resources.
ChRM, characteristic remanent magnetization: a stable vector (=straight and defined by ≥4 demagnetization steps).

[a] A_5 is a 95% confidence region about a Paleopole on the surface of the globe. However, the confidence region is more precisely described by an elliptical area on the globe's surface. The angular dimensions of its axes are (dP and dM, e.g., Table 2 for our paleopoles). Approximately, $A_{95} = \sqrt{(dM \times dP)}$.

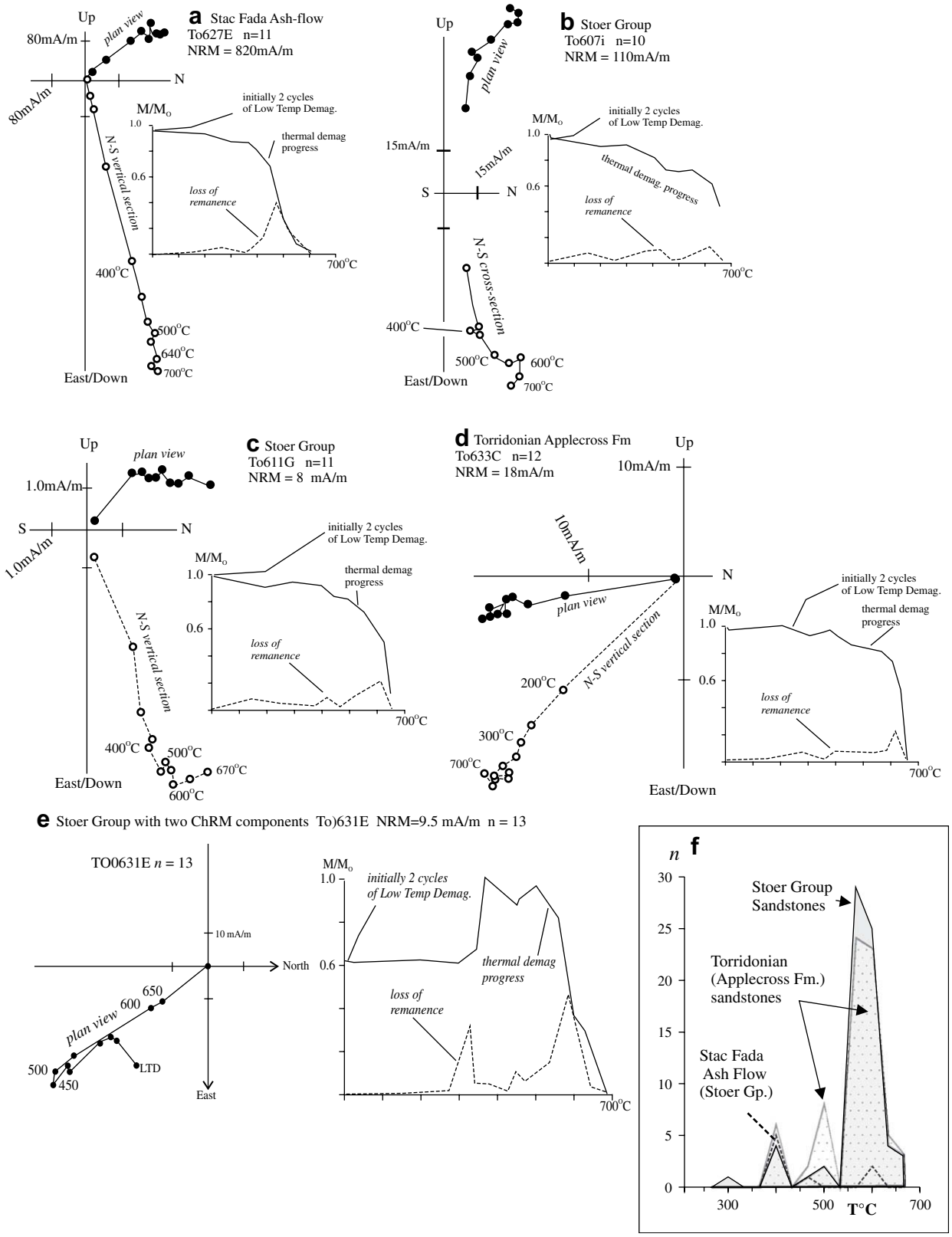

Fig. 12. (a–d) Vector plots (with intensity-decay graphs inset) for typical specimens. Note that most specimens show a single characteristic remanence component (ChRM); its direction is typically NW-down for the Stoer Group and SE-down for the Torridon Group. However, some reverse directions are recorded due to Proterozoic geomagnetic polarity reversals. (e) Some Stoer Group specimens reveal that the SE-down vector of the younger Torridon Group is superimposed on Stoer Group sedimentary rocks as a remagnetization event. (f) Frequency distribution of unblocking temperatures (T_{UB}) for ChRMs in general.

1989, 1991) since the RBM do not behave as passive markers freely spinning in the straining rock matrix (Borradaile, 1991a,b). Moreover the remanence may be partly demagnetized, and remagnetized, during ephemeral stresses at very small shortening stains (<8%) (Borradaile, 1996; Borradaile and Jackson, 1993; Jackson et al, 1993). Fortunately, the Stoer and Torridon groups show negligible penetrative strain although AMS identified a cryptic N–S vertical embryonic tectonic foliation (Figs. 7–9). AMS fabrics, which align RBMs as well as matrix minerals postdate flexures of bedding in the Stoer and Torridon Groups. Clearly, the magnetizations carried by the RBMs must postdate deposition, diagenesis and the vertical N–S tectonic microfabric. Other authors emphasized that the paleomagnetic signals are largely carried by secondary specular hematite (Irving, 1957; Torsvik and Sturt, 1987) and it is well known that in red-beds of any age, hematization may be much later than deposition (Butler, 1992).

7. Demagnetization experiments

Differently oriented components of magnetization, of different age sum to yield a mostly useless direction, referred to as the Natural Remanent Magnetization (NRM). Some suitable laboratory strategy is adopted for isolating and determining the relative historical value of the differently oriented magnetic vectors that constitute NRM (Schmidt, 1993). Stewart (2002) noted that a full paleomagnetic interpretation of this area awaited sufficient samples with full demagnetization experiments. NRM often, as here, includes a young viscous component due to the present earth's field during the Bruhnes' epoch; e.g. northward-seeking or Normal polarity over the last 0.7 Ma, inclined appropriately for the site. Even less relevant spuriously oriented weak magnetic components are acquired during handling and transport. Low-temperature demagnetization (LTD), in which the sample is cooled in liquid Nitrogen and allowed to warm back to room temperature inside a magnetic shield (Dunlop and Özdemir, 1997), usually removes any such vectors that have no geological importance. Subsequently, careful progressive thermal demagnetization experiments isolate earlier vector directions known as the characteristic remanence (ChRM) directions. The pre-treatment by low-temperature cycling is beneficial here because it will enhance the resolution of turning points between different ChRMs due to overlapping coercivity spectra between the grains that carry different vector components (Hoffman and Day, 1978; Dunlop, 1979; Halls, 1979). Commonly, pre-treatment by LTD cycling usually clarifies the distinction between vector components and sharpens turning pints on vector plots (Borradaile et al., 2001a, 2004).

Ten to 14 steps of thermal demagnetization were performed between 150 and 675 °C or 700 °C. After each step, remanence was re-measured and interactive vector plots permitted identification of unblocking temperatures (T_{UB}) that separated ChRM vectors (e.g., Fig. 12a–e). Whereas, the minerals' Curie/Néel temperatures dictate the ultimate (T_{UB}), geological history determines lower T_{UB}s, the general frequency distribution for which is shown in Fig. 12f. These locate the end-point of ChRM vectors which define ancient geomagnetic field directions.

Changes in vector orientation during demagnetization correspond to significant orientations of the paleofield with respect to the specimen. Two important directions are found; NW-down in the Stoer Group (Fig. 12a–c) and SE-down in the Torridon Group (Fig. 12d). Some Stoer Group rocks contain both vectors, with the SE-down component as a stable "Torridon age" overprint on the NW-down component (Fig. 12e). These concur with earlier predictions, though here we have fully demagnetized every specimen and the sample sizes are much larger than previously used and our precision is higher (Table 2). Both components show an equal range of unblocking temperatures in different specimens and presumably correspond to different ages of remagnetization or hematite neocrystallization. Both directions may be found equally overprinting the underlying gneissic basement where they are usually carried by magnetite and, as one would expect for imprints in complexly recrystallized rock, they are not always chronologically distinct (e.g., Piper, 1987, 1992a,b). However, Piper and Poppleton (1991) suggested a pre-Stoer age for similar ChRM directions in the basement. The characteristic NW-down magnetization for Stoer deposition, and the subsequent SE-down for the Torridonian deposition reside in chemically precipitated specular hematite (Irving, 1957) which may be produced during notoriously long post-depositional neo-mineralization events, broadly termed chemical remanent magnetization (CRM Butler, 1992). We shall see below that both directions, while dominant in each of the Stoer and Torridon Groups, is accompanied also by reversed magnetization directions. Before proceeding to evaluate the geological importance of the ChRM vectors from paleomagnetic data, we should recall that the AMS fabrics, which include RBM minerals, postdate the undulations of Stoer and Torridon strata, defining an N–S vertical foliation. Thus, the RBM mineral fabric postdates the buckling and diagenesis of the strata.

If ChRM vectors are not dispersed by the differently inclined parts of a fold, the magnetization postdates folding and cannot be primary. However, by definition, any fold involving limb-curvature or variation in layer thickness has also suffered (heterogeneous) finite strain. We may correct for the effects of rigid-body tilting (MacDonald, 1980) but it is impossible to correct for the effects of

Table 2
Summary of paleomagnetic results from this work

		n ChRM vectors	Raw (in situ) mean ChRM vector		Tilt-corrected mean vector (Scot. Coord.)		α_{95}	Rotated into Laurentian coordinates			Paleopole confidence region	
								Paleopole		Paleo-latitude		
			Decl.	Incl.	Decl.	Incl.		Latitude	Longitude		d*m*	d*P*
Torridon Gp. (Applecross Fm.)	Applecross	42	138.4	52.2	124.7	43.8	7.4	−30.2	213.1	−25.6	6.8	3.9
	Culkein N.	15	134.9	45.5	124.4	36.8	16	−25.1	213.9	−20.5	15.1	8.2
	Balchl. N.	19	134.4	55.1	129.2	45.8	11.3	−31.4	208.3	−27.2	10.2	5.8
Stoer Group	*Stoer Gp.*	*49*	*317.0*	*43.1*	*331.8*	*43.5*	*11.3*	*29.5*	*191.1*	*29.5*	*9.6*	*5.8*
	Stoer Gp.	*23*	*309.9*	*52.1*	*330.0*	*58.6*	*10.6*	*36.6*	*194.1*	*39.3*	*7.7*	*5.5*
	Stoer Gp. ("Torridon" overprints)	19	133.3	52.5	120.4	43.2	9.6	−30.0	217.7	−25.1	9.1	5
	StacFada Ash[a]	*9*	*292.2*	*62.3*	*320.7*	*72.2*	*9.2*	*53.6*	*206.2*	*57.3*	*5.1*	*4.7*
	Balchl. S	*43*	*314.6*	*44.5*	*330.1*	*50.4*	*7.4*	*20.9*	*206.7*	*31.1*	*6.4*	*3.8*

Values in italics are for data with NW trending vectors (normal polarity paleofield). Values in roman for data with SE trending vectors (reversed polarity paleofield). α_{95}, radius of Fisher (1953) confidence region in degrees; d*m*, d*P*, radii of confidence region (A_{95}) for paleopole; Regional un-tilting is about axis 015/00, 12° clockwise; Euler rotation of Scottish paleopoles into Laurentian coordinates uses Bullard rotation axis at Longitude/Latitude 088/27 with anticlockwise rotation of 36°; Balchl, Balcladdich.

[a] Low paleomagnetic significance since secular variation may be poorly averaged at this site.

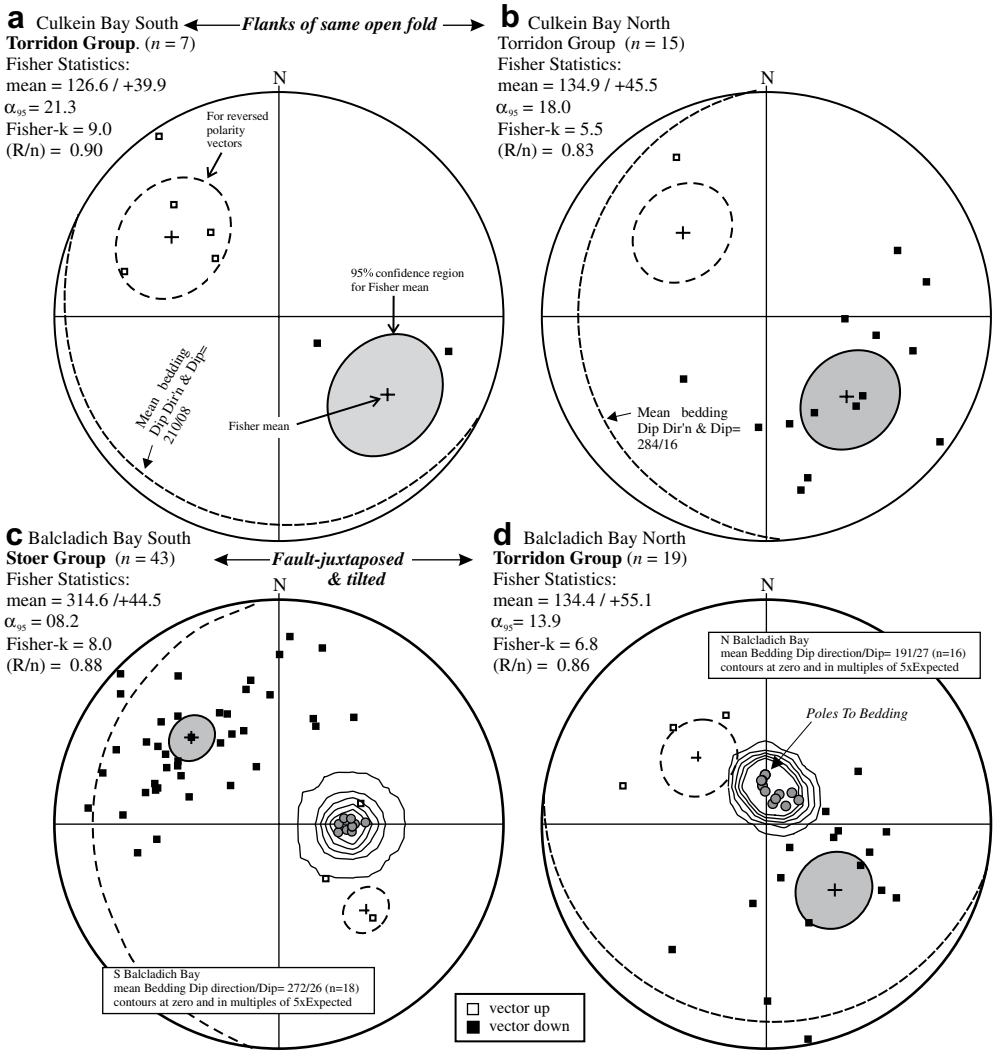

Fig. 13. "Tilt-tests". In each stereogram, the Fisher mean for the dominant group of characteristic (ChRM) vectors is shown surrounded by its 95% confidence region. In each stereogram a few vectors are approximately antiparallel to the main ChRM direction (close to the mirror image of the Fisher confidence region on the opposite hemisphere, indicated with a broken line). These vectors represent magnetizations by reversed polarity paleofields. (a–b) Near Culkein (Fig. 2) adjacent sites on opposite flanks of an open warp of bedding yield ChRM vectors; mean bedding planes shown. The mean ChRM directions from the two flanks are indistinguishable using the test (Fisher et al., 1987, p. 208); this indicates that the magnetizations postdate the tilting and warping of the red-beds. (c–d) At Balcladdich (Fig. 2) oppositely tilted Stoer and Torridon Group red-beds yield mean ChRM directions parallel to those found elsewhere in differently and less steeply dipping Stoer and Torridon red-beds, respectively (e.g. Figs. 18, 19). This further supports the late chemical magnetization of both Stoer and Torridon red-beds, during the burial of each Group respectively, long after deposition.

strain (Borradaile, 1997) so that the "fold test" must be viewed with some caution. We tested open folds (actually round-hinge warps, not chevrons) of Torridon sandstone (Fig. 13a–b). They possess a well-defined SE-down direction, with some reversed magnetization vectors due to paleofield reversal(s). The vectors are not convincingly deflected in accordance with the fold flanks. Therefore, the ChRMs appear to postdate tilting (it fails the tilt-test) and they were acquired over a long interval, including at least one palaeofield polarity transition.

At Balcladdich Bay, opposed dips of the Stoer Group and Torridon Applecross Group occur due to tilting on either side of a SW–NE fault (Fig. 2). NW-down vectors in the Stoer Group (Fig. 13c) and SE-down vectors in the Torridon Group, on the other side of the fault, retain the same directions as elsewhere in the region, regardless of the dip of their host beds. Thus the typical NW-down Stoer direction and SE-down Torridon direction are clearly post-tilting magnetizations. Again, both were acquired slowly enough to trap paleofield reversals (Fig. 13c–d).

For the Stoer Group on the Stoer peninsula, uniformly tilted sandstone strata yield consistent normal polarity (Fig. 14a) and reverse-polarity (Fig. 14b) Stoer-directions. These high precision mean direction agree well with the other mean vectors for the Stoer Group (Table 2). The Stac Fada Ash Flow within the Stoer Group yields a small sample of ChRM vectors (Fig. 14c). Ash flow magnetite is unlikely to average secular variation, hence the scatter and slight disagreement with the Stoer NW-down ChRM direction (Fig. 14c).

Torridon Group ChRM vectors are presented for sites with uniformly inclined bedding (Stoer peninsula Fig. 15a) and for the Stoer Group (between Clachtoll and Culkein; Fig. 15b). These replicate the NW-down Stoer vector and SE-down Torridon Group vector, with quite large samples (23 and 42 sites). Both samples show some sites with reversed polarity confirming the slow magnetization process and the consistency of the paleofield's mean direction. For regional comparison, 11 sites in the Torridon Group along the coast from south of Stoer to Cape Wrath at the NW tip of Scotland verify the SE-down vector for the Torridon Group (Fig. 15c). (Regional comparisons cannot be made for the Stoer Group because of its much more limited geographic distribution.) All of the paleomagnetic data are documented in Table 2 which indicates rather high precision and consistency for mean vectors of

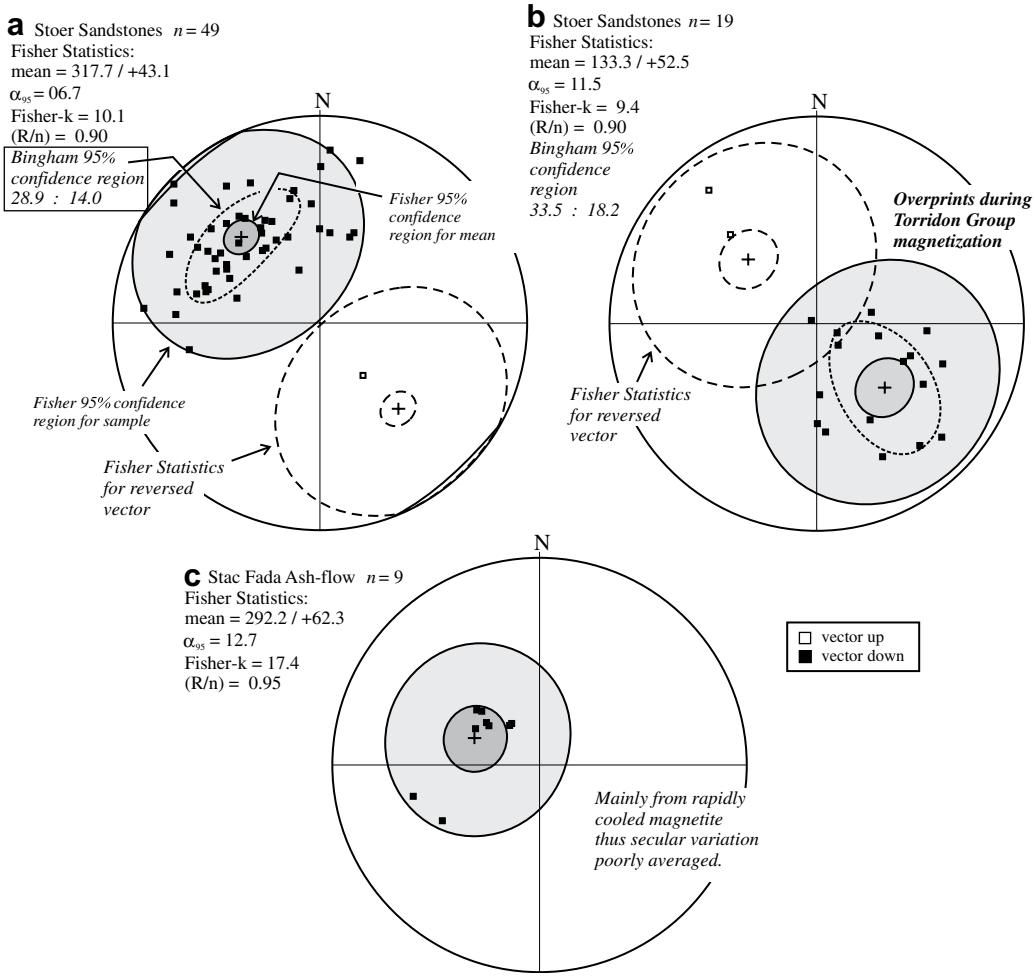

Fig. 14. ChRM directions from Stoer Group. (a) Most common directions for the Group point NE-down with precisely defined vector mean from large sample (i.e. small confidence region about the mean direction). The 95% confidence region for the sample (lighter shade) is also shown, as well as the elliptical confidence region for the mean assuming a Bingham (1963) rather than a circular-normal Fisher (1953) distribution. A few antiparallel vectors indicate magnetization during a reversed polarity epoch, indicating the long duration of the magnetization processes. (b) For the Stoer Group, the dominant ChRM vectors point SE-down, again with some reverse field vectors indicating long duration chemical magnetization. (c) Like the rest of the Stoer Group, the Stac Fada ash flow shows ~NW-down ChRM vectors but this direction differs significantly from the Stoer red-beds; this is attributed to the remanence being borne mainly by rapidly cooled magnetite which failed to average out paleosecular variation. Thus, this direction will locate a virtual geomagnetic pole (VGP), rather than a reliable time-averaged paleopole.

both the Stoer and Torridon Groups. Intra-group agreement of Fisher means is satisfactory at the 95% level using the test of Fisher et al. (1987, p. 208).

Red-beds have the ability to record remanence over a long period of time, as shown by the presence of reversed polarity signals in every sample of each Group, general knowledge of remanence carried by specular hematite and specific earlier observations here (Butler, 1992; Irving, 1957; Torsvik and Sturt, 1987). In contrast, sampling the Stac Fada Ash flow, within the Stoer Group, yields a slightly discordant paleofield direction since it has less successfully averaged palaeosecular variation.

The Stoer and Torridon Group sandstones provide consistent high precision mean directions (Table 2), suggesting the magnetization process successfully averaged secular variation. Thus, meaningful paleopoles should be defined from the Stoer and Torridon Group ChRM directions. The fundamental question is of course, are these ChRMs *primary*, i.e. syn-depositional? van der Voo (1993) reminds us that primary age is the most fundamental criterion for establishing the value of a paleopole (Table 1); however, this is invariably the most difficult criterion to satisfy. Usually and at best, one or both age limits may be bracketed by field tests (Graham, 1949; Everitt and Clegg, 1962). Here, our strongest argument for the diagenetic age of the ChRM is that they include paleo-reversals. In each sample of the Stoer and Torridon Groups, a few vectors are antiparallel to the prominent vector mean (Figs. 13–15). Antiparallel vectors in all cases lie in the mirror image of the sample's 95% confidence region, indicating reasonable symmetry of the reversals. Although the number of reversals is convincing in itself, their precision is inadequate to determine if the paleofield reversal(s) were symmetric or not. Asymmetry has been detected in this and other Proterozoic intervals (Pesonen and Halls, 1983; Schmidt and Williams, 2003). For our purposes, it suffices to note that chemical magnetization processes endured for long intervals; post-dating bed-warping, during burial and diagenesis, and sampling geomagnetic field reversals. Our sample sizes and precision satisfy van der Voo's (1993) quality requirements and provide circumstantial support for the longevity of the magnetization process: the high precision (worst α_{95} is $<16^{\circ}$; Table 2) indicates that the variance of secular variation was successfully suppressed. By Phanerozoic standards this would require an interval of much more than 0.1 Ma and probably several Ma.

Laboratory storage tests exclude the possibility of any important viscous magnetization (Irving and Runcorn, 1957). However, the magnetizations may be at least co-diagenetic for the following reasons. First, the classic "conglomerate" field test (Graham, 1949) verifies the stability of the Stoer and Torridon remanences since

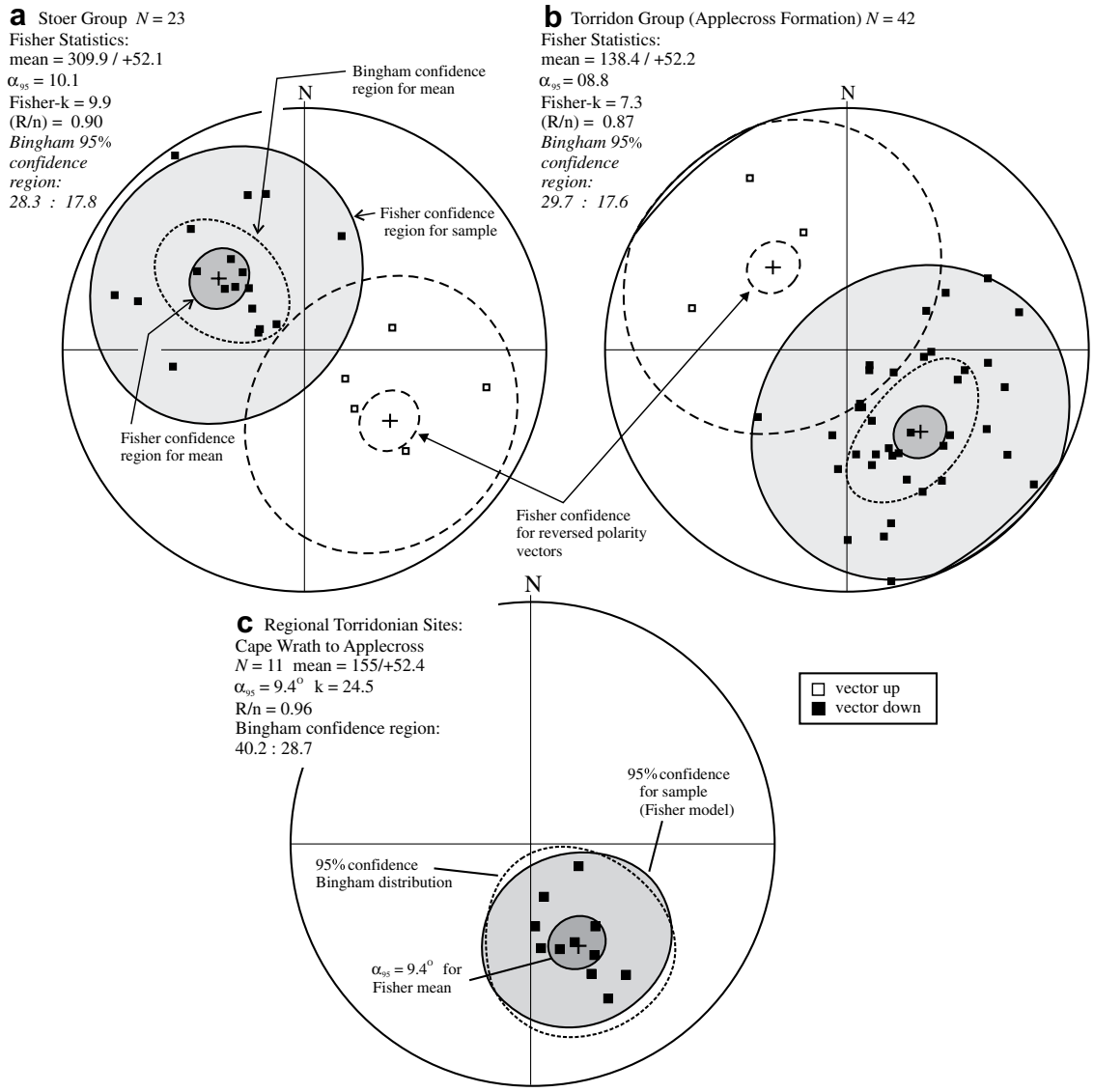

Fig. 15. ChRM directions from further samples of Stoer and Torridon Group red-beds. From the Stoer peninsula, the mean ChRM vectors are precisely defined; (a) NW-down for the Stoer Group; (b) SE-down for the Torridon Group. In each case, palaeoreversals are represented by a few antiparallel vectors, testifying to a long post-depositional chemical magnetization. The Torridon Group vectors postdate and overprint the Stoer Group vectors in some Stoer sites. (c) Beyond the Stoer peninsula, 11 sites along the NW Scottish coast, close to the eastern boundary fault of the Proterozoic rift all yield SE-down ChRMs for the Torridon Group (Applecross Formation) red-beds. These sites also bear NW–SE vertical tectonic AMS sub-fabrics.

their clasts have scattered remanences when re-deposited in Permian conglomerate (Irving and Runcorn, 1957; "positive conglomerate test"). Second, Proterozoic intra-formational clasts scatter retain scattered Proterozoic remanence vectors (Torsvik and Sturt, 1987). Third, although surprisingly overlooked, since Stewart's discovered that the Stoer Group is unconformably overlain by the Torridon Group, the difference in their principal ChRM directions indirectly implies a primary age for Stoer Group magnetization. Fourth, one of the simplest arguments that the ChRMs are ancient and enduring occurs where samples are sufficiently large, as here. These sample sizes are sufficient to record reversals of the paleofield for both the Stoer and Torridon Groups. Since the stability of geomagnetic polarity is measured in millions of years this is as powerful as a classic field-test of ChRM stability (van der Voo, 1993; here Table 1). The magnetization processes were long enough to span at least one polarity transition since antiparallel ChRM vectors were found in both Stoer and Torridon Groups. Moreover, the presence of antiparallel vectors in the same stratigraphic Groups and even the same sites provides strong evidence for a "nearly" primary age. Fifth, Stoer and Torridon Group magnetizations are retained in clastic dikes causally associated with paleo-rift faulting (Dulin et al., 2005), again implying their primary age.

Before proceeding, we emphasize that *primary* in paleomagnetic sense, is less specific than in structure or sedimentology. Chemical remanent magnetization (CRM) is generally regarded as a long duration process, especially in red-beds where hematite may crystallize over a large interval of the diagenetic and burial history (Darabi and Piper, 2004; Torsvik and Sturt, 1987).

8. Paleomagnetic interpretation

Fortunately, penetrative strain does not appear to have affected the Torridon and Stoer ChRMs. Of course, there are embryonic tectonic overprints revealed by the vertical N–S AMS foliation; this is more severe near the Caledonian front, just 20 km to the east. Fortunately, there is no possibility of confusion the Proterozoic ChRMs with syntectonic Caledonian remagnetization (End-

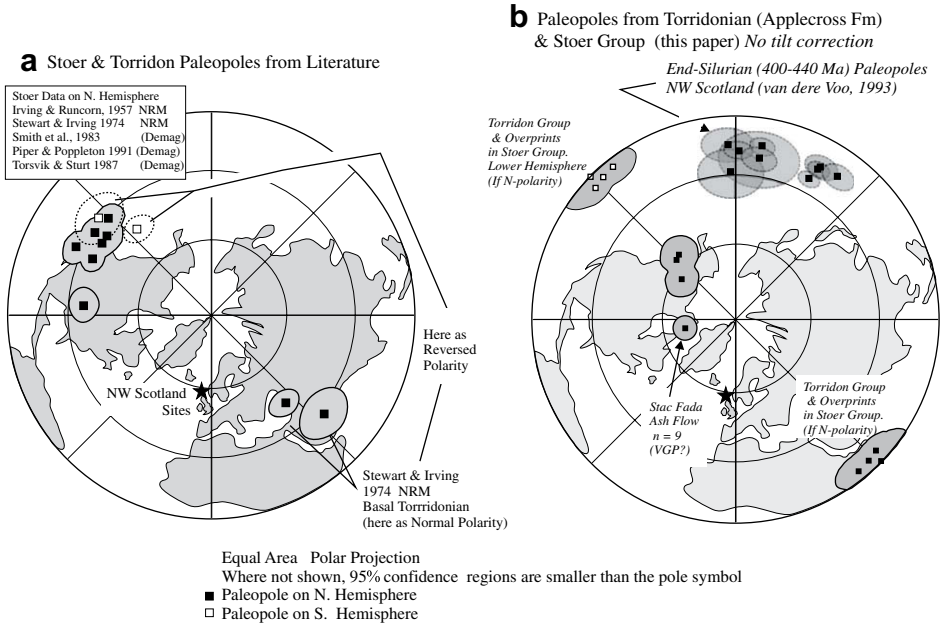

Fig. 16. (a) Previously published Proterozoic paleopoles for the Stoer and Torridon Groups. Differences with our results (shown later) may result from different (or no) demagnetization procedures and different tilt-correction procedures. (b) Our raw paleopoles (no tilt corrections) are first compared in Scottish coordinates to the paleopoles imprinted on the adjacent Caledonian orogen during its end-Silurian. Thus we may reject any argument that Caledonian remagnetization affected the Proterozoic rocks, essentially strain-sheltered in the Proterozoic Hebridean rift.

Silurian, ~420 Ma) since the palaeopole positions are quite different (Fig. 16; after van der Voo, 1993, Table A2).

Stoer and Torridon ChRMs postdate the local fold or fault-induced tilting and therefore *local tilt* corrections are inappropriate. However, the entire foreland has been significantly tilted on a regional scale shown by the dip of the Cambrian erosion surface. It is not clear if this correction has been applied in earlier studies. We back-rotated the characteristic paleomagnetic vectors using this regional tilt-axis, re-computing modern locations of paleopoles gives relative to NW Scotland (Fig. 17a).

For comparison with other parts of the Laurentian supercontinent (Rodinia) the Scottish paleopoles are rotated into Laurentian coordinates using the accepted Euler rotation axis (Fig. 17b). In Laurentian coordinates, the Stoer paleopoles lie in the NW Pacific and in Torridon poles lie in the eastern Mediterranean (Fig. 17b). The Torridon Group SE-down vectors are anomalous, unless we accept that they were acquired in a reverse palaeofield. In that case, their paleopoles lie more appropriately in the Pacific, compatible with other Laurentian Proterozoic rocks (Fig. 17b).

9. Paleomagnetic data compared

The Proterozoic of NW Scotland and its Lewisian basement are part of the Laurentian component of the Proterozoic

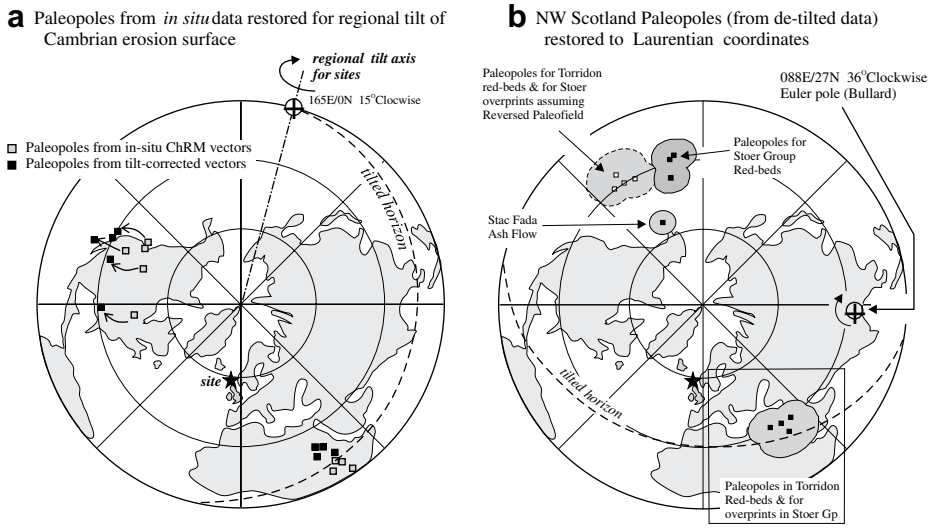

Fig. 17. (a) Our mean ChRM vectors were de-tilted, correcting for the regional tilt of the Cambrian erosion surface. Since the ChRM vectors, due to late burial chemical remagnetization, postdate local tilt variations, we have not corrected for such features. (b) The paleopoles are then restored into Laurentian coordinates using the Euler rotation axis shown. Paleopoles due to SE-down ChRM vectors, in the Torridon Group and due to Torridon age remagnetization of the Stoer Group produce anomalous locations in the eastern Mediterranean. If we assume these were produced during a reversed polarity epoch, their paleopole locations shift to the south-central Pacific, which is in agreement with our and other data (Fig. 18) for the Laurentian Shield.

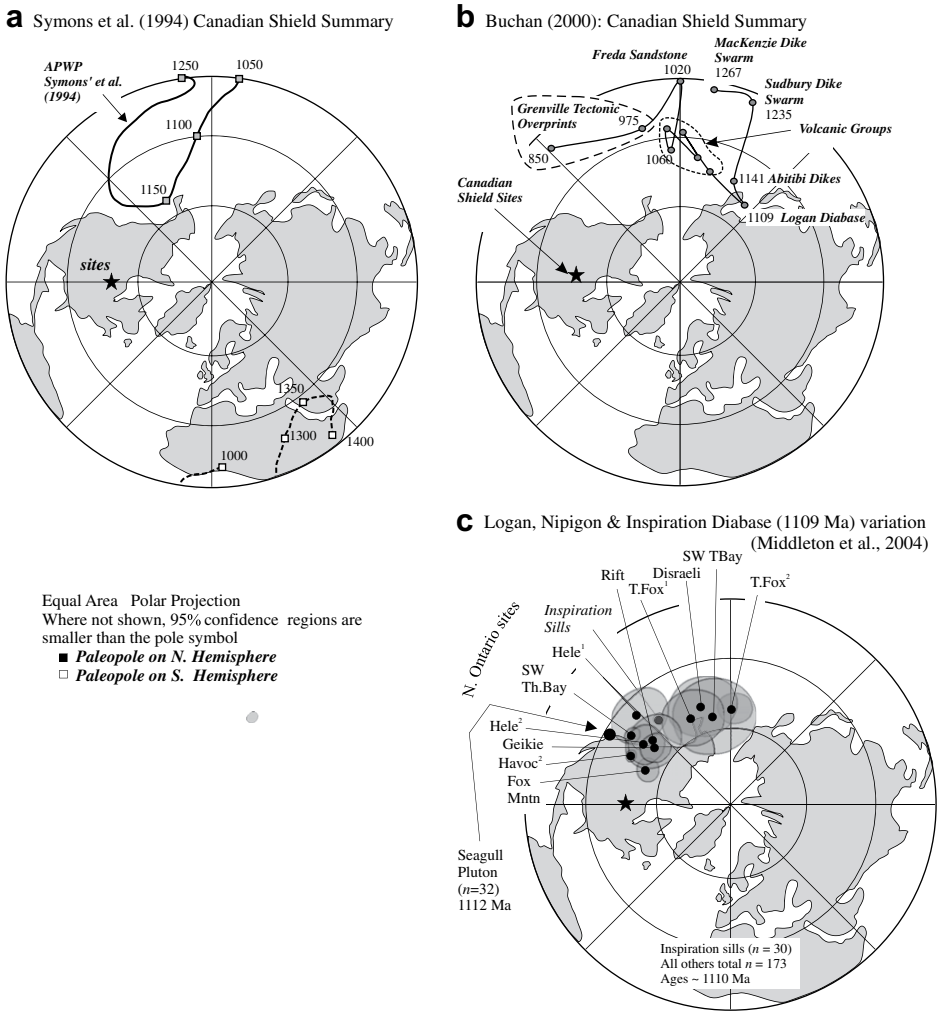

Fig. 18. Published paleopole positions, some with ages that permit the definition of an apparent polar wander path (APWP). (a) Symons et al. (1994) widely accepted track, with the Logan "hairpin bend" near ~1100 Ma due to the Grenville tectonic event (Fig. 1) which caused a change in the direction of terrain/microplate motion. (b) APWP due to (Buchan et al., 2000). (c) Certain recent precise data suggest the Laurentian APWP track should have the hairpin bend located in western North America, closer to Symons' synthesis in (a).

Supercontinent Rodinia. Thus, Stoer and Torridon paleomagnetic data are compared with Canadian data in the Canadian reference frame. Most Superior craton paleopoles of the Canadian Shield have coeval, precise radiometric ages (Costanzo-Alverez and Dunlop, 1988; Symons et al., 1994; Buchan et al., 1996, 2000, 2001, 1993; Middleton et al., 2004). However, the NW Scottish Proterozoic has a paucity of geochronologically suitable rocks. Younger Proterozoic Laurentian data, from the Superior craton are summarized along a dated *apparent polar wander path* (APWP) in Fig. 18. Buchan et al. (2000) also provides a more precisely dated partial APWP for the older Proterozoic. Most relevant is the Middle and Late Proterozoic APWP to which some adjustments due to recent palaeomagnetic or geochronologic data. For example, recent findings locate the northern hairpin bend in the APWP loop closer to Alaska at ~1000 Ma (Fig. 18c). The poorly defined, youngest part of the APWP (~800 Ma) may turn northward toward the central Pacific at ~700 Ma (Weil et al., 1998; Piper, 1991, 1992a,b, 2000).

Our Stoer and Torridon paleomagnetic data differ slightly from earlier studies and agree more closely with the Laurentian AWP. First, every specimen has been subject to at least 10 steps of incremental thermal demagnetization, providing very stable ChRM vectors. Second, every specimen was exposed to ≥2 cycles of low-temperature demagnetization (LTD, Dunlop and Özdemir, 1997). This pre-treatment sharpens the turning points between important paleomagnetic vectors in subsequent thermal demagnetization. Third, we did not apply *local* tilt corrections since we have shown that magnetic fabrics (expressed by RBM) and paleomagnetic vectors postdate the gentle dip variations and open folds. However, did restore the obvious *regional* eastward tilt shown by the Cambrian erosion surface.

Paleopoles for the Stoer and Torridon Groups are distinct from those acquired in the Caledonides, <10 km to the East (Fig. 16b). However, Caledonian orogenic remagnetization or overprinting (420–440 Ma) is known in the region and Blumstein et al. (2005) found some Paleozoic magnetizations in the Torridonian.

ChRM vectors are NW-down for the Stoer Group and SE-down for the Torridon Group. If both directions were due to Normal polarity paleofields, the uncorrected paleopoles lie in western North America and the Eastern Mediterranean, respectively (Fig. 17b). Correcting these ChRMs for the post-Cambrian regional tilt of the Stoer and Torridon Groups displaces paleopoles southward and northward, respectively (Fig. 17b). This gives different locations from those determined by others using local (site-specific) tilt corrections. Of course, to interpret these paleopoles in a suitable paleogeographic frame of reference, the Hebridean craton and its paleopoles must be rotated into contiguity with the Laurentian craton (Fig. 17b) using the Euler pole for the

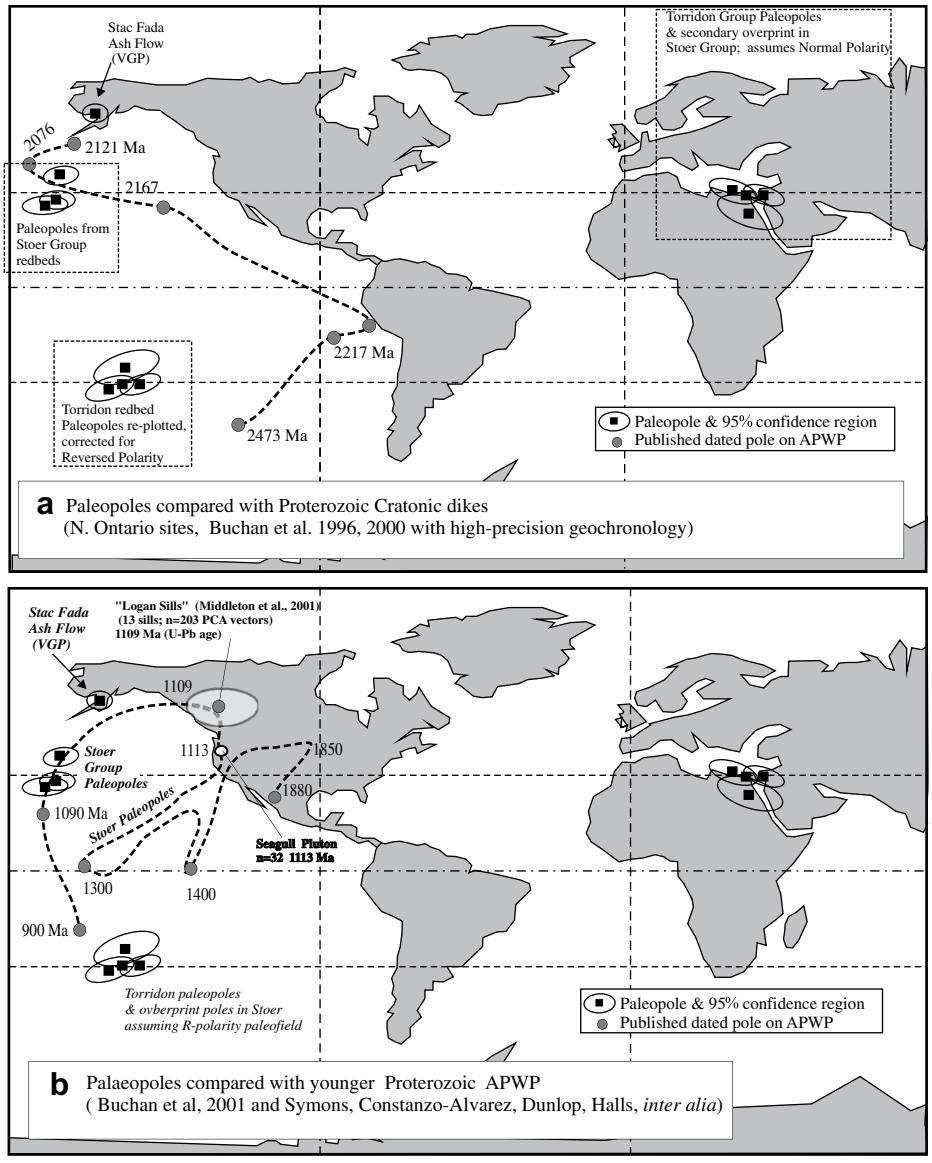

Fig. 19. The principal APWP literature from the data is shown for the (a) Early and (b) Later Proterozoic of the restored Rodinian supercontinent (Fig. 1), in Laurentian coordinates. The most rational interpretation of the Torridon Group paleopoles requires their generation in a reversed field, giving present paleopole locations in the south-central Pacific. The Stoer paleopoles lie in the north-central Pacific. Locations on the APWP, using dates for other paleopoles imply ages of ~1100 and 900 Ma for the late chemical magnetizations of the Stoer and Torridon Groups, respectively. Paleolatitude differences indicate therefore that latitudinal displacement rates were in the range 27–40 km/Ma.

reconstruction of these parts of the Rodinia Supercontinent (Piper, 1987). Thus, the corrected Stoer paleopoles now lie in the present-day Pacific ~190°E/25°N whereas the Torridon paleopoles lie in the eastern Mediterranean. The latter location is untenable with any paleogeographic reconstruction unless we accept that the Torridon paleopoles were generated during reversed geomagnetic polarity. Thus, their paleopoles lie more logically in the south-central Pacific at ~210°E/25°S.

10. Conclusions and paleomagnetic interpretation

Both the Stoer Group and overlying Torridon Group show a range of magnetic fabric orientations, carried both by matrix forming minerals and remanence-bearing accessory minerals. AMS principal axes may define depositional fabrics when plotted in bedding coordinates with k_{MAX} and k_{INT} parallel to bedding. However, both Stoer and Torridon Group red-beds show a transitional tectonic fabric with an NS or NW–SE cryptic tectonic foliation, in which k_{MAX} trends N–S. The tectonic imprint is better developed east of the Stoer peninsula where it is enhanced by proximity to the Caledonian orogenic front. However, in the Stoer peninsula, the AMS cryptotectonic fabrics are apparently Proterozoic since they are accompanied by pre-Caledonian remanent magnetization. As in the Mid-continental Proterozoic rift of the Superior craton, the embryonic tectonic fabrics are due to rift margin displacements.

Chemical magnetization of the Stoer Group red-beds occurred after warping, fault-related tilting, and during an extensive interval of diagenesis and burial that bracketed paleofield reversals and many cycles of secular variation. The ancient, characteristic components of the remanence are also unaffected by the cryptic tectonic fabrics which were revealed by AMS. The tectonic AMS fabrics appear related to rift-fault orientations and may have formed prior to magnetization. The importance of the magnetizations is indicated by polarity transitions and successful averaging of secular variation; these require an interval of at least 0.1 Ma and may well have encompassed several million years. The red-bed magnetization of the unconformably overlying Torridon also postdates its local bed-warping, successfully averages secular

variation and spanned at least one geomagnetic reversal, indicating a similar long duration diagenetic-burial processes of chemical magnetization. Stoer and Torridon paleopoles, in uncorrected Scottish coordinates, do not correlate with typical during Caledonian orogenic remagnetization (~440 Ma) (Fig. 16b).

Site-specific tilt corrections for the paleomagnetic ChRM vectors are inappropriate since the vectors are not dispersed according to the beds' orientations; indeed remanences were acquired after the N–S vertical microfabric which aligns the RBM. However, we did correct for the later regional tilt shown by the gradient of the Cambrian erosion surface (Fig. 17a). ChRM vectors were subsequently restored into Laurentian coordinates to compensate for the net continental drift, using an accepted Euler rotation pole for the reassembly of the Hebridean and Laurentian craton (Fig. 17b). The recomputed paleopoles lie on the Laurentian APWP, with the Stoer Group paleopoles approximately between 1000 and 1110 Ma along the track (Fig. 19b). This is somewhat younger than a Pb–Pb limestone isotopic age from the Stoer Group which is in the range 1129–1269 Ma (Turnbull et al., 1996). The common ChRM vector for the Torridon Group is directed SW-down which after restoration yields paleopoles that lie in the eastern Mediterranean. This also includes a set of secondary magnetizations in the Stoer Group acquired at similar times. The alternative interpretation is that the dominant geomagnetic fields during Torridon Group deposition were reversed, so that the paleopoles have a more rational location in the south-central Pacific, on the Laurentian APWP near the published poles dated at 850–900 Ma (Fig. 19b). This is somewhat younger than the Rb-Sr phosphate age range of 946–1042 Ma, determined from the Torridon Group (Turnbull et al., 1996). Our paleopole positions agree more closely with the published APWP tracks (Fig. 19b) and differ from earlier publications. This is in part because our sample sizes were larger, producing higher precision but chiefly because we found local tilt corrections were inappropriate whereas a regional tilt correction was necessary. The age and paleopole locations for the Torridon Group are also indirectly corroborated by the paleofield reversals since paleofield reversals are well documented during Keewenawan igneous activity 1008–1115 Ma (e.g., Middleton et al., 2004; Pesonen and Halls, 1983) in the Lake Superior region (Fig. 1).

The Stoer Group burial magnetization occurred considerably after diagenesis, microfabric development and flexures of bedding. The ChRM indicates the Stoer rocks then lay at paleolatitudes between 26°N and 44°N (95% confidence $\leq 10°$). Results from the Stoer Group's Stac Fada ash flow may not average secular variation (Tables 1 and 2) and thus yield an unreliable "virtual" geomagnetic pole position and an unrealistic paleolatitude (Fig. 17b). Subsequently, Torridon Group magnetized after burial and microfabric development, faulting and bed-flexuring. It was then situated between 23°S and 27°S (95% confidence $\leq 15°$) (Table 2). Accepting Turnbull et al.'s (1996) isotopic age ranges for the Stoer and Torridonian; the craton must have moved southward at rates between 27 and 40 km/Ma. This paleomagnetic argument only invokes the *latitudinal* component of displacement; longitudinal components of motion are probable and imply higher net displacement rates dependent on the azimuth of motion.

Acknowledgments

The Natural Sciences and Engineering Research Council of Canada (NSERC, Ottawa) continuously funded GB between 1978 and 2006. This funded the present and many related projects. Catherine Borradaile assisted at all stages of the fieldwork, without which help this project would not have been completed. Dr. R. Douglas Elmore and Dr. P.A. Cawood provided careful and helpful reviews for which we are very grateful.

References

Bingham, C., 1963. Distributions on the sphere and on the projective plane. PhD thesis, Yale University.
Blumstein, R.D., Elmore, R.D., Engel, M.H., Parnell, J., Baron, M., 2005. Multiple fluid migration events along the Moine Trust Zone, Scotland. Journal of the Geological Society 162, 1031–1045.
Borradaile, G.J., 1987. Anisotropy of magnetic susceptibility: rock composition versus strain. Tectonophysics 138, 327–329.
Borradaile, G.J., 1988. Magnetic susceptibility, petrofabrics and strain. Tectonophysics 156, 1–20.
Borradaile, G.J., 1991b. Correlation of strain with anisotropy of magnetic susceptibility (AMS). Pure and Applied Geophysics 135, 15–29.
Borradaile, G.J., 1991a. Remanent magnetism and ductile deformation in an experimentally deformed magnetite-bearing limestone. Physics of the Earth Planet and Planetary Interiors 67, 362–373.
Borradaile, G.J., 1993. Strain and magnetic remanence. Journal of Structural Geology 15, 383–390.
Borradaile, G.J., 1996. Experimental stress remagnetization of magnetite. Tectonophysics 261, 229–248.
Borradaile, G.J., 1997. Deformation and paleomagnetism. Surveys in Geophysics 18, 405–435.
Borradaile, G.J., 2001a. Magnetic fabrics and petrofabrics: their orientation distributions and anisotropies. Journal of Structural Geology 23, 1581–1596.
Borradaile, G.J., 2001b. Paleomagnetic vectors and tilted dikes. Tectonophysics. 333, 417–426.
Borradaile, G.J., 2003. Statistics of Earth Science Data. Springer-Verlag, Berlin, Heidelberg & New York, 351 pp.
Borradaile, G.J., Gauthier, D., 2003. Interpreting anomalous magnetic fabrics in ophiolite dikes. Journal of Structural Geology 25, 171–182.
Borradaile, G.J., Henry, B., 1997. Tectonic applications of magnetic susceptibility and its anisotropy. Earth Science Reviews 42, 49–93.
Borradaile, G.J., Jackson, M., 1993. Changes in magnetic remanence during simulated deep sedimentary burial. Physics of the Earth Planet and Planetary Interiors 77, 315–327.
Borradaile, G.J., Jackson, M., 2004. Anisotropy of magnetic susceptibility (AMS): magnetic petrofabrics of deformed rocks. In: Martin-Hernandez, F., Lünenburg, C.M., Aubourg, C., Jackson, M. (Eds.), Magnetic Fabric: Methods and Applications. Geological Society London, Special Publication, vol. 238, pp. 299–360.
Borradaile, G.J., Mothersill, J.S., 1989. Tectonic strain and paleomagnetism: experimental investigation. Physics of the Earth Planet and Planetary Interiors 56, 254–265.
Borradaile, G.J., Mothersill, J.S., 1991. Experimental strain of isothermal remanent magnetisation in ductile sandstone. Physics of the Earth Planet and Planetary Interiors 65, 308–318.
Borradaile, G.J., Sarvas, P., 1990. Magnetic susceptibility fabrics in slates: structural, mineralogical and lithological influences. Tectonophysics 172, 215–222.
Borradaile, G.J., MacKenzie, A., Jensen, E., 1990. Silicate versus trace mineral susceptibility in metamorphic rocks. Journal of Geophysics Research 95, 8447–8451.
Borradaile, G.J., Tarling, D.H., 1981. The influence of deformation mechanisms on the magnetic fabrics of weakly deformed rock. Tectonophysics 77, 151–168.
Borradaile, G.J., Keeler, W., Alford, C., Sarvas, P., 1987. Anisotropy of magnetic susceptibility of some metamorphic minerals. Physics of the Earth Planet and Planetary Interiors 48, 161–166.
Borradaile, G.J., Lagroix, F., Trimble, D., 2001. Improved isolation of archeomagnetic signals by combined low temperature and alternating field demagnetization. Geophysical Journal International 147, 176–182.
Borradaile, G.J., Lucas, K., Middleton, R.S., 2004. Low-temperature demagnetization isolates stable vector components in magnetite-bearing diabase. Geophysical Journal International 157, doi:10.1111/j.1365-246X.2004.02201.x.
Buchan, K.L., Mortensen, J.K., Card, K.D., 1993. Northeast-trending Early Proterozoic dykes of southern Superior Province: multiple episodes of emplacement recognized from integrated paleomagnetism and U-Pb geochronology. Canadian Journal of Earth Science 30, 1286–1296.
Buchan, K.L., Halls, H.C., Mortensen, J.K., 1996. Paleomagnetism, U–Pb geochronology, and geochemistry of Marathon dykes, Superior Province, and comparison with the Fort Francis swarm. Canadian Journal of Earth Sciences 33, 1583–1595.
Buchan, K., Ernst, R.E., Hamilton, M.A., Mertanen, S., Pesonen, L., Eming, S-Å., 2001. Rodinia: the evidence from integrated paleomagnetism and U–Pb geochronology. Precambrian Research 110, 9–32.
Buchan, K.L., Mertanen, S., Park, R.G., Pesonen, L.J., Elming, S.-Å., Abrahamsen, N., Bylund, G., 2000. Drift of Laurentia and Baltica in the Proterozoic: the importance of key Paleomagnetic poles. Tectonophysics 319, 167–198.
Butler, R.F., 1992. Paleomagnetism: Magnetic Domains to Geologic Terranes. Blackwell, Oxford, 319 pp.
Costanzo-Alverez, V., Dunlop, D.J., 1988. Paleomagnetic evidence for post-2.55-Ga tectonic tilting and 1.1-Ga reactivation in the Southern Kapuskasing Zone, Ontario, Canada. Journal of Geophysical Research 93, 9126–9136.
Daly, L., Zinsser, H., 1973. Étude comparative des anisotropies de susceptibilité et d'aimantation rémanente isotherme: conséquences pour l'analyse structurale et le paléomagnétisme. Annales de Géophysique 29, 189–200.
Darabi, M.H., Piper, J.D.A., 2004. Palaeomagnetism of the (late Mesoproterozoic) Stoer Group, northwest Scotland; implications for diagenesis, age and relationship to the Grenville Orogeny. Geological Magazine 2004 (141), 15–39.

Davis, D.W., Sutcliffe, R.H., 1985. U–Pb ages from the Nipigon "Plate" (sic) and northern Lake Superior. Geological Society of American Bulletin. 96, 1572–1579.
Downie, C., 1962. So-called spores from the Torridonian. Geological Society of London, Proceedings 160, 127–128.
DuBois, P.M., 1960. Paleomagnetism and correlation of Keweenawan Rocks. Geological Survey of Canada, Bulletin 71, 75 pp.
Dulin, S., Elmore, R.D., Engel, M.H., Parnell, J., Kelly, J., 2005. Palaeomagnetic dating of clastic dykes in Proterozoic basement, NW Scotland; evidence for syndepositional faulting during deposition of the Torridonian. Scottish Journal of Geology 41, 149–157.
Dunlop, D.J., 1972. Magnetic mineralogy of heated and unheated red sediments by coercivity spectrum analysis. Geophysical Journal. Royal Astronomical Society 27, 37–55.
Dunlop, D.J., 1979. On the use of Zijderveld vector diagrams in multicomponent paleomagnetic studies. Physics of the Earth and Planetary Interiors 20, 12–24.
Dunlop, D.J., Özdemir, Ö, 1997. Rock Magnetism: Fundamentals and Frontiers. Cambridge Studies in Magnetism. Cambridge University Press, 573 pp.
Everitt, C.W.F., Clegg, J.A., 1962. A field test of paleomagnetism stability. Geophysical Journal of the Royal Astronomical Society 6, 312–319.
Ferré, E.C., 2002. Theoretical models of intermediate and inverse AMS fabrics. Geophysical Research Letters 29 (7), 31–41.
Fisher, N.I., Lewis, T., Embleton, B.J.J., 1987. Statistical Analysis of Spherical Data. Cambridge University Press, 329 pp.
Fisher, R.A., 1953. Dispersion on a sphere. Proceedings of Royal Society A217, 295–305.
Franklin, J.M., McIlwaine, W.H., Poulsen, K.H., Wanless, R.K., 1980. Stratigraphy and depositional setting of the Sibley Group, Thunder Bay District, Ontario, Canada. Canadian Journal of Earth Sciences 17, 633–651.
Graham, J.W., 1949. The stability and significance of magnetism in sedimentary rocks. Journal of Geophysical Research 54, 131–167.
Green, J.C., 1983. Geologic and Geochemical Evidence for the Development of the Middle Proterozoic (Keweenawan) Midcontinent Rift of North America. In: Morgan, P., Baker, B.H. (Eds.), Processes of Continental Rifting. Tectonophysics 94, 413–437.
Halls, H.C., 1979. Separation of multicomponent NRM: combined use of difference and resultant magnetization vectors. Earth and Planetary Science Letters 43, 303–308.
Halls, H.C., Pesonen, L.J., 1982. Paleomagnetism of Keweenawan Rocks. Geological Society of America Memoir 56, 173–201. Chapter 9.
Henry, B., 1989. Magnetic fabric and orientation tensor of minerals in rocks. Tectonophysics 165, 21–28.
Hoffman, K.A., Day, R., 1978. Separation of multi- component NRM: a general method. Earth and Planetary Science Letters 40, 433–438.
Holm, D.K., Darrah, K.S., Lux, D.R., 1998. Evidence for widespread ~1760 Ma metamorphism and rapid crustal stabilization of the early Proterozoic (1870–1820 Ma) Penokean orogen, Minnesota. American Journal of Sciences 298, 60–81.
Hrouda, F., 1982. Magnetic anisotropy of rocks and its application in geology and geophysics. Geophysical Surveys 5, 37–82.
Irving, E., 1957. The origin of the paleomagnetism of the Torridonian sandstones of North-West Scotland. Philosophical Transactions of Royal Society of London A250, 100–110.
Irving, E., McGlynn, J.C., 1981. On the coherence, rotation and paleolatitude of Laurentia in the Proterozoic. In: Kröner, A. (Ed.), Precambrian Plate Tectonics. Elsevier Publishing Company, Amsterdam, pp. 561–598.
Irving, E., Runcorn, S.K., 1957. Analysis of the paleomagnetism of the Torridonian sandstones series of North-West Scotland. Philosophical Transactions of Royal Society of London A250, 83–99.
Jackson, M., 1991. Anisotropy of magnetic remanence: a brief review of mineralogical sources, physical origins, and geological application, and comparison with susceptibility anisotropy. Pure and Applied Geophysics 136, 1–28.
Jackson, M., Borradaile, G.J., Hudleston, P.J., Banerjee, S.K., 1993. Experimental deformation of synthetic magnetite-bearing calcite sandstones: effects on remanence, bulk magnetic properties, and magnetic anisotropy. Journal of Geophysical Research 98, 383–401.
Jelinek, V., 1978. Statistical processing of anisotropy of magnetic susceptibility measured on groups of specimens. Studia Geophysica et Geodaetica 22, 50–62.
Kinnaird, T.C., Prave, A.R., Kirkland, C.L., Horstwood, M., Parrish, R., Batchelor, R.A., 2007. The late Mesoproterozoic–early Neoproterozoic tectonostratigraphic evolution of NW Scotland: the Torridonian revisited. Journal of Geological Society of London 164, 541–551, doi:10.1144/0016-76492005-096.
MacDonald, W.D., 1980. Net tectonic rotation, apparent tectonic rotation, and structural tilt correction in paleomagnetic studies. Journal of Geophysical Research 85, 3659–3669.
McElhinny, M.W., McFadden, P.L., 2000. Paleomagnetism, Continents and Oceans. Academic Press, 386 pp.
Middleton, R.S., Borradaile, G.J., Baker, D., Lucas, K., 2004. Proterozoic diabase sills of northern Ontario: magnetic properties and history. Journal of Geophysical Research 109, B02103, doi:10.1029/2003JB002581, 12 pp.
Nakamura, N., Borradaile, G.J., 2001a. Strain, anisotropy of anhysteretic remanence, and anisotropy of magnetic susceptibility in a slaty tuff. Physics of the Earth Planet and Planetary Interiors 125, 85–93.
Nakamura, N., Borradaile, G.J., 2001b. Do reduction spheroids predate finite strain? A magnetic diagnosis of Cambrian slates in North Wales. Tectonophysics 304, 133–139.
Nakamura, N., Borradaile, G.J., 2004. Metamorphic control of magnetic susceptibility and its fabric anisotropies: a 3-D projection. In: Martin-Hernandez, F., Lünenburg, C.M., Aubourg, C., Jackson, M. (Eds.). Magnetic Fabric: Methods and Applications, Geological Society London, pp. 61–68. Special Publication 238.
Paces, J.B., Miller, J.D., 1993. Precise U–Pb ages of Duluth complex and related mafic intrusions, northeastern Minnesota: geochronological insights to physical, petrogenetic, paleomagnetic and tectonomagmatic processes associated with the 1.1 Ga Midcontinent Rift system. Journal of Geophysical Research 98, 13997–14013.
Pesonen, L.J., Halls, H.C., 1983. Geomagnetic field intensity and reversal asymmetry in late Precambrian Keweenawan rocks. Geophysical Journal of Royal Astronomical Society 73, 241–270.
Piper, J.D.A., 1991. Paleomagnetism and the Continental Crust. J. Wiley & Sons, 434 pp.
Piper, J.D.A., 1987. The paleomagnetic record in the Lewisian terrain. In: Park, R.G., Tarney, J. (Eds.), Evolution of the Lewisian and Comparable High-grade Terrains. Geological Society Special Publications, vol. 27, pp. 205–215.
Piper, J.D.A., 1992a. Post-Laxfordian magnetic imprint in the Lewisian metamorphic complex and strike-slip motion in the Minches, NW Scotland. Journal of Geological Society London 149, 127–137.
Piper, J.D.A., 1992b. The paleomagnetism of major (Middle Proterozoic) igneous complexes, outh Greenland and the Gardar apparent polar wander track. Precambrian Research 54, 153–172.
Piper, J.D.A., 2000. The Neoproterozoic Supercontinent: Rodinia or Paleopangea. Earth and Planetary Science Letters 176, 131–146.
Piper, J.D.A., Poppleton, T.J., 1991. Conglomerate tests on basal Stoer Group sedimentary rocks, NW Scotland. Scottish Journal of Geology 27, 97–106.
Potter, D.K., Stephenson, A., 1988. Single-domain particles in rocks and magnetic fabric analysis. Geophysical Research Letters 15, 1097–1100.
Rainbird, R.H., Hamilton, M.A., Young, G.M., 2001. Detrital zircon geochronology and provenance of the Torridonian, NW Scotland. Journal of the Geological Society 158, 15–27.
Robertson, W.A., 1973. Pole position from thermally cleaned Sibley Group sediments and its relevance to Proterozoic magnetic Stratigraphy. Canadian Journal of Earth Sciences 10, 180–193.
Robertson, W.A., Fahrig, W., 1971. The great Logan paleomagnetic loop – the polar wandering path from Canadian Shield rocks during the Neohelikian Era. Canadian Journal of Earth Sciences 8, 1355–1372.
Robion, P., Borradaile, G.J., 2001. Stress remagnetization in pyrrhotite–calcite synthetic aggregates. Geophysical Journal International 144, 96–104.
Rochette, P., 1987. Magnetic susceptibility of the rock matrix related to magnetic fabric studies. Journal of Structural Geology 9, 1015–1020.
Rochette, P., 1988. Inverse magnetic fabric in carbonate-bearing rocks. Earth and Planetary Science Letters 90, 229–237.
Rochette, P., Jackson, M., Aubourg, C., 1992. Rock magnetism and the interpretation of anisotropy of magnetic susceptibility. Review of Geophysics 30, 209–226.
Schmidt, P.W., 1993. Paleomagnetic cleaning strategies. Physics of the Earth Planet and Planetary Interiors 76, 169–178.
Schmidt, P.W., Williams, G.E., 2003. Reversal asymmetry in Mesoproterozoic overprinting of the 1.88 Ma Gunflint Formation, ONtario, Canada: non-dipole effects or apparent polar wander? Tectonophysics 377, 7–32.
Stewart, A.D., 2002. The Later Proterozoic Torridonian Rocks of Scotland: Their Sedimentology, Stratigraphy, Geochemistry and Origin. In: Geological Society of London Memoir, No. 24, 130 pp.
Stewart, A.D., Irving, E., 1974. Paleomagnetism of Precambrian sedimentary rocks from NW Scotland and the apparent polar wandering path of Laurentia. Geophysical Journal of Royal Astronomical Society 37, 51–72.
Sutcliffe, R.H., 1991. Proterozoic Geology of the Lake Superior Area. In: Thurston, P.C., Williams, H.R., Sutcliffe, R.H., Stott, G.M. (Eds.), Geology of Ontario, pp. 627–658. Part 1.
Symons, D.T.A., Lewchuk, M.T., Dunlop, D.J., Costanzo-Alverez, V., Halls, H.C., Bates, M.P., Palmer, H.C., Vandall, T.A., 1994. Synopsis of paleomagnetic studies in the Kapuskasing structural zone. Canadian Journal of Earth Sciences 31, 1206–1217.
Tarling, D.H., Hrouda, F., 1993. The MaS200gnetic Anisotropy of Rocks. Chapman & Hall, London, 217 pp.
Thomas, D.N., Piper, J.D.A., 1992. A revised magneto-stratigraphy for the Mid-Proterozoic Gardar lava succession, South Greenland. Tectonophysics 201, 1–16.
Torsvik, T.H., Sturt, B.A., 1987. On the origin and stability of remanence and the magnetic fabric of the Torridonian Red Beds, NW Scotland. Scottish Journal of Geology 23, 23–38.
Turnbull, M.J.M., Whitehouse, M.J., Moorbath, S., 1996. New isotopic age determinations for the Torridonian, NW Scotland. Journal of Geological Society of London 153, 955–964.
van der Voo, R., 1993. Paleomagnetism of the Atlantic, Tethys and Iapetus Oceans. Cambridge University Press, Cambridge, 411 pp.
Weil, A.B., Van der Voo, R., MacNicaill, C., Meert, J.G., 1998. The Proterozoic Supercontinent Rodinia: paleomagnetically derived reconstructions for 1100 to 800 Ma. Earth & Planetary Science Letters 154, 13–24.
Werner, T., Borradaile, G.J., 1996. Paleoremanence Dispersal across a transpressed Archean Terrain: deflection by anisotropy or by late compression? Journal of Geophysical Research 10, 5531–5545.